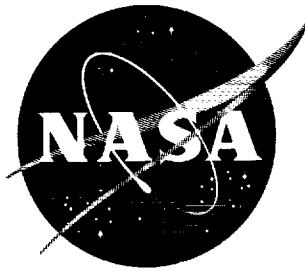# TECHNICAL NOTE
D-321

FLIGHT INVESTIGATION OF THE LOW-SPEED CHARACTERISTICS

OF A 45° SWEPT-WING FIGHTER-TYPE AIRPLANE WITH

BLOWING BOUNDARY-LAYER CONTROL APPLIED TO

THE LEADING- AND TRAILING-EDGE FLAPS

By Hervey C. Quigley, Seth B. Anderson,
and Robert C. Innis

Ames Research Center
Moffett Field, Calif.

NATIONAL AERONAUTICS AND SPACE ADMINISTRATION

WASHINGTON   September 1960

NATIONAL AERONAUTICS AND SPACE ADMINISTRATION

TECHNICAL NOTE D-321

FLIGHT INVESTIGATION OF THE LOW-SPEED CHARACTERISTICS

OF A 45° SWEPT-WING FIGHTER-TYPE AIRPLANE WITH

BLOWING BOUNDARY-LAYER CONTROL APPLIED TO

THE LEADING- AND TRAILING-EDGE FLAPS

By Hervey C. Quigley, Seth B. Anderson,
and Robert C. Innis

SUMMARY

A flight investigation has been conducted to study how pilots use the high lift available with blowing-type boundary-layer control applied to the leading- and trailing-edge flaps of a 45° swept-wing airplane. The study includes documentation of the low-speed handling qualities as well as the pilots' evaluations of the landing-approach characteristics. All the pilots who flew the airplane considered it more comfortable to fly at low speeds than any other F-100 configuration they had flown. The major improvements noted were the reduced stall speed, the improved longitudinal stability at high lift, and the reduction in low-speed buffet.

The study has shown the minimum comfortable landing-approach speeds are between 120.5 and 126.5 knots compared to 134 for the airplane with a slatted leading edge and the same trailing-edge flap. The limiting factors in the pilots' choices of landing-approach speeds were the limits of ability to control flight-path angle, lack of visibility, trim change with thrust, low static directional stability, and sluggish longitudinal control. Several of these factors were found to be associated with the high angles of attack, between 13° and 15°, required for the low approach speeds. The angle of attack for maximum lift coefficient was 28°.

INTRODUCTION

Previous flight research on the use of boundary-layer control (BLC) on swept wings has been concerned mainly with BLC applied to trailing-edge flaps in conjunction with "mechanical" type devices for controlling leading-edge flow separation. When used on highly deflected leading- and trailing-edge flaps, BLC can delay leading-edge flow separation to high angles of attack and lift coefficients, as well as provide large flap lift increments. The maximum lift is larger than can be achieved

by purely mechanical means, such as slats, slots, etc. In applications of boundary-layer control to increase maximum lift, an important question before the designer is how much of this increased lift available at high angles of attack will the pilot be able to use. Therefore the aircraft which had been studied previously in reference 1 in connection with BLC applied to trailing-edge flaps was modified to provide BLC on the leading-edge flaps as well as on the trailing-edge flaps.

This report presents the results of an investigation designed to study how pilots use the high lift available with blowing boundary-layer-control leading- and trailing-edge flaps, to provide operation experience on this type of an installation, and to determine the limiting factors in the choice of landing approach speed when wing stall is delayed to high angles of attack.

NOTATION

b	wing span, ft
BLC	boundary-layer control
C_D	drag coefficient
C_L	lift coefficient
$C_{L_{max}}$	maximum lift coefficient
C_μ	momentum coefficient
$C_{1/2}$	number of cycles for oscillation to damp to half amplitude
F	control force, lb
g	acceleration of gravity, 32.2 ft/sec^2
h_p	pressure altitude, ft
MAC	mean aerodynamic chord
N	engine speed, percent
p	rolling velocity, radians/sec
P	period, sec
q	free-stream dynamic pressure, lb/ft^2

T	engine thrust, lb
V	velocity, knots
w	weight flow of engine bleed air, lb/sec
W	gross weight, lb
α	angle of attack, deg
β	sideslip angle, deg
ΔT	increment of military thrust available
δ	ratio of total pressure at compressor to standard sea-level pressure
δ_a	aileron deflection, deg
δ_f	flap deflection, deg
δ_t	horizontal-tail deflection, deg
θ	ratio of total temperature at compressor to standard-sea-level temperature
φ	bank angle, deg
$\dfrac{|\varphi|}{|V_e|}$	amplitude ratio of the angle of bank to equivalent side velocity in the oscillatory mode, deg/ft/sec

Subscripts

i	indicated
A	approach
LE	leading edge
TE	trailing edge
s	stall

EQUIPMENT AND TESTS

Airplane

A 45° swept-wing fighter-type airplane (modified F-100A) was used as the test vehicle for this investigation. A two-view sketch of the airplane is shown in figure 1 and a photograph of the airplane during landing is shown in figure 2. Table I presents the geometric data for the test airplane.

Leading-Edge Flap

The leading-edge flap was a plain type with a blowing nozzle on the flap radius. Figure 3 is a photograph of the flap mounted on the test airplane. The flap design was based on the results of reference 2 and was constructed at Ames Research Center. Figure 4(a) is a typical cross section showing pertinent dimensions. The flap deflection was adjusted by the use of flap position links of various lengths; the range of adjustment was from 0° to 60°. The nozzle was fixed and located 30° from a line normal to the chord line. The nozzle gap was nominally 0.015 inch but could be adjusted by adding or removing shims. Figure 4(b) is a sketch of the plan form showing the spanwise extent of the three separate flaps. The flap chord varied from 8.8 percent (inboard) to 16.6 percent (outboard) of the streamwise chord.

Trailing-Edge Flap

The airplane was equipped with the boundary-layer-control trailing-edge flap described in reference 1 but the nozzle was modified to maintain a nearly constant gap at all duct pressures.

Ducting and Bleed Air

Bleed air for BLC was ducted from the last stage of engine to the root of both the leading- and trailing-edge flaps. Figure 5 is a sketch of the ducting showing the position of the control valves, etc. The ducting to the leading-edge flap was external from the engine compartment to the wing root as shown in figure 6. Since the ducting crossed the wheel wells, the landing gear could not be retracted. Ducting to the trailing-edge flap was all internal.

Control of bleed air to both the leading- and trailing-edge flaps was by separate butterfly valves driven by geared electric motors. Indicators in the cockpit showed the pilot the duct pressures at each wing tip and at the trailing-edge flap. The pilot could adjust duct pressure to any desired setting or set the switches for automatic duct pressure regulation. In the automatic position of the switch, duct pressures were maintained between 40 and 45 psig in the leading-edge and between 45·and 50 psig in the trailing-edge flap. The weight flow of bleed air extracted from the engine for BLC is shown in figure 7 for the valve both fully open and automatically controlled. The quantity of bleed air used for leading-edge BLC is shown separately in figure 7(b).

Figure 8 shows the static thrust loss due to the quantity of bleed air indicated in figure 7. It can be seen that the automatic regulation of duct pressure reduced the thrust loss appreciably at high engine speeds. To increase the thrust at low speed, the radius of the engine inlet leading edge was increased from 1/2 inch to 1-1/2 inches. Figure 9 is a photograph of the modification. The increased radius raised the pressure recovery of the inlet which resulted in an 11-percent increase in static thrust at maximum engine speed.

Instrumentation and Test

Standard NASA recording instruments were used for measuring airspeed, altitude, angle of attack, normal and longitudinal acceleration, roll, pitch and yaw rates of angular velocity and tail-pipe pressure. An oscillograph was used to record angle of sideslip; left and right aileron, flap, rudder, and throttle position; and duct pressures. A photo panel recorded engine speed, tail-pipe and free-air temperatures, and fuel used.

The flight tests were conducted between sea level and 15,000 feet and between 200 knots and minimum flight speeds. The take-off wing loading was 64.4 pounds per square foot and landing wing loading was 55 pounds per square foot. The center of gravity varied between 0.318 to 0.294 mean aerodynamic chord for these changes in wing loading. The leading-edge flap deflection used for this investigation was 40° inboard and 60° midspan and outboard. (See fig. 4(b).) Boundary-layer control was applied only to the midspan and outboard leading-edge flaps. The trailing-edge flap deflection was either 0° or 45° with BLC.

RESULTS AND DISCUSSION

The most important result of the tests is considered to be the effect that leading-edge BLC has on the pilots' choices of landing-approach speeds and on the landing-approach characteristics in general. The appendix is a discussion of the lift and drag effects of the leading-edge BLC flap.

With the leading-edge BLC flap the pilots reported improvements in the general handling qualities over the complete low-speed range (200 knots to stall). All the pilots who flew the airplane considered it more comfortable to fly at low speed than any F-100 configuration they had flown. The major improvements noted were the reduced stall speed, the improved longitudinal stability at high lift, and the reduction in low-speed buffet. The stall speed was reduced about 10 knots as a result of the leading-edge BLC flap, while the angle of attack for stall was increased 7.5^O. However, flying at these higher angles of attack and low airspeeds resulted in some handling qualities problems as will be discussed later along with the pilots' evaluations of the landing-approach characteristics. Included also is the effect of the leading-edge BLC flap on various low-speed handling qualities. In the evaluation of the landing-approach and low-speed handling qualities, the pilots used the standard rating system noted in table II.

Landing-Approach Evaluation

The airplane was flown by three Ames pilots. Carrier-type approaches were made in order to eliminate as many variables in the approach as possible. The mirror landing aid could not be used because of the lack of visibility at high angles of attack. For this reason flat, continuous, turning approaches were made with little or no straightaway. Two of the pilots (A and B) evaluated the airplane under conditions of moderate turbulence. These pilots chose a slightly higher minimum comfortable approach speed than the third pilot whose evaluation was conducted in smooth air. The approach speed chosen by each pilot is tabulated in table III. Included in the table for comparison purposes are the approach speeds obtained with the slatted leading edge and the same trailing-edge flap (ref. 1). In general, the pilots felt that the handling qualities of the airplane with the BLC leading-edge flap were improved over those of the airplane with the slatted leading edge. This is reflected by their willingness to reduce their approach speed as indicated in table III. All the pilots agreed that the primary factor that prevented further reduction in approach speed was the limits of their ability to control longitudinal flight path or arrest a sink rate. However, there were several secondary factors which influenced their choice of approach speed and these will be discussed separately.

As mentioned earlier, visibility was a factor at the high attitudes used in the approach. In figure 10 the minimum comfortable approach speeds have been converted to C_L and are marked on a C_L - α curve. It can be seen from these data that approach angles of attack as high as 15° were used. At these high angles as altitude was reduced, the pilot's view of the ground was obstructed and his visual cues pertaining to flight-path angle and point of touchdown were progressively reduced. This lack of visibility undoubtedly impaired the pilot's ability to control flight-path angle and, although none of the pilots regarded it as a primary

reason for limiting approach speed, it must be considered a secondary factor. No attempt was made to determine the speed at which visibility was considered satisfactory. At these high approach angles of attack the airplane attitude was above the maximum ground attitude of the airplane, that is, the angle between the center line of the airplane and the ground when the wheel (oleos extended) and tail skid were just touching the ground (fig. 11). The pilots commented that they realized they were approaching above maximum ground attitude, but this was not a limiting factor in their choice of approach speed, since contact with the ground was not required for the evaluation, or if contact with the ground was imminent, a push-over could be made to a smaller angle at touchdown.

Another secondary factor that the pilots considered limiting was the adverse trim change with abrupt thrust change. This characteristic shown in time-history form in figure 12(a) indicates that as thrust was increased, the initial response of the airplane was a decrease in angle of attack, an increase in airspeed, and a slight decrease in altitude. All of these initial response characteristics were considered adverse by the pilots since the pilots desired a nose-up change in flight-path angle for an increase in thrust with little change in airspeed and angle of attack (ref. 3). It is of interest to note that, as shown in figure 12(b), the horizontal-tail angle required to trim to 130 knots does not change with thrust. However, the angle of attack required to trim to 130 knots decreased as thrust was increased. (Computations have shown that at high angles of attack the lift component of thrust is large, requiring a change in aerodynamic lift as thrust is changed to maintain a constant airspeed.) It appears, therefore, that at this speed the pitching-moment change due to thrust change is about equal but opposite to the pitching-moment change due to angle-of-attack change. The change in angle of attack excites the phugoid mode of the longitudinal oscillation (fig. 12(a)), resulting in a large increase in airspeed. The period of the phugoid is so long (32 seconds per cycle) that only the first few seconds of the phugoid motion affect the landing approach characteristics. More research is required to fully define the airplane response to an abrupt throttle motion which will be considered satisfactory by the pilot.

The two stability and control factors listed by the pilots as secondary reasons for limiting approach speed were the low directional stability and the longitudinal control power becoming inadequate. The pilots felt that both directional stability and control decreased with airspeed, hence, their rating of the directional stability and control changes from 5 at 130 knots to 6 at 120 knots. However, the directional stability as determined by the rudder required for steady-state sideslip (fig. 13) was nearly constant; that is, $d\beta/d\delta_R$ does not change appreciably with speed, indicating the pilot desired greater static directional stability and control at high angles of attack and low airspeed. At the high angles of attack the airplane rolls about its inclined axis, producing a sideslip angle proportional to angle of bank. In figure 14 it

is shown graphically that in aileron rolls the sideslip as computed by the relationship $\beta = \alpha_0 \sin \varphi$ is nearly equal to the measured values of β. The higher the angle of attack the higher will be the sideslip due to roll. The pilots considered these sideslip values rather large and objectionable. At the lower approach speeds the pilots felt the longitudinal control power was sluggish. Figure 15 shows that as airspeed was decreased $d\delta_t/dV$ became more negative, indicating larger control motions are required for a given change in airspeed. Although this would appear to the pilot as a decrease in longitudinal control power, computations have shown that the control effectiveness is nearly constant over the C_L range used during the approach. Figure 15 compares the measured values of $d\delta_t/dV$ with the computed value assuming a constant dC_m/dC_L. These data indicate the change in $d\delta_t/dV$ is due to an increase in static longitudinal stability. Wind-tunnel studies (ref. 2) have shown that part of the increase in stability at the higher angles of attack results from the contribution of the horizontal tail to the static stability. The static longitudinal stability was considered by the pilots to be good (a numerical rating of 2) and greatly improved by the leading-edge BLC flap.

The thrust available for maneuvering ($\Delta T/W$) was not a limiting factor as it was for the slatted leading-edge configuration (ref. 1); however, it was considered by the pilots to be low. Figure 16 shows that with the present configuration $\Delta T/W$ was 0.11 as compared to 0.045 for the slatted leading-edge configuration. (A $\Delta T/W$ of 0.12 was considered minimum in ref. 4.) The gain in $\Delta T/W$ resulted from the decrease in drag and an increase in available thrust. The greater thrust available was obtained by modifying the engine inlet (fig. 9) and by minimizing the thrust loss due to bleed air by automatically controlling the bleed air used for BLC.

Figure 16 and table III show that the pilot's approach speeds, V_A, for both the slatted and the BLC leading-edge flap are a little below the speed for minimum drag.

It appears there may be an upper limit on the angle of attack usable in landing approach. It is believed that the present configuration was being operated near this limit. This was brought out in two ways. First, with the leading-edge BLC flap, flow over the wing was improved and stall speed was reduced appreciably, but the ratio of approach speed to stall speed, V_A/V_S, was as high as 1.31. This ratio is high in comparison with other swept-wing configurations (ref. 5). Second, although the primary reason for limiting approach speed was the inability to control the longitudinal flight path, the secondary reasons were all associated with the high attitude except the longitudinal control power deterioration. Several of the secondary factors which limited approach speed were similar to some of the factors found in the investigation of the low-speed handling qualities of a delta-wing airplane (ref. 6) which operated at equal or higher angles of attack in the landing approach. Three of these common factors were adverse trim change with thrust, sideslip due to roll about the inclined longitudinal axis, and low directional stability.

It is felt that for an airplane to utilize fully the high lift gains of BLC leading-edge flaps, the wing angle of attack in the landing approach will have to be reduced by very effective trailing-edge flaps, drooped ailerons, or other means.

Low-Speed Handling Qualities

Static longitudinal stability.- The static longitudinal stability as indicated by the variation of horizontal-tail angle with lift coefficient is shown in figure 17 for various configurations. The data show that with the nose flap alone $(C_{\mu_{LE}} = 0)$, as C_L is increased, stability becomes neutral, then abruptly negative, followed by another abrupt change to positive stability. Tuft studies indicated that the initial pitch-up is associated with wing tip stalling that progresses inboard. With increasing $C_{\mu_{LE}}$ the C_L for neutral stability is moved to higher C_L values and the change in stability becomes less abrupt. At a $C_{\mu_{LE}}$ value of about 0.015 and above, the stability is positive over the whole C_L range.

Trim changes due to leading-edge BLC.- The trim change associated with the application of leading-edge BLC is shown in figure 18 for three airspeeds. The data show that large pull forces would be required if BLC were turned on at an airspeed of 130 knots or below. At 150 knots the trim force is within the 10 pounds required by military specifications. However, turning the BLC on at any speed was not considered objectionable by the pilot, as he felt that in so doing he was improving his situation by the elimination of separation on the wing with its associated unsteadiness, buffet, and high drag. The trim change itself was hardly noticed. On the other hand turning BLC off at any speed below 160 knots gave the impression the airplane was stalling and pitching and resulted in an uncomfortable feeling.

Dynamic longitudinal stability.- The period and damping of the short period longitudinal oscillation variation with airspeed are shown in figure 19. The period and time to damp to half amplitude $(T_{1/2})$ increase as speed is decreased. The pilots considered the period and damping of the short-period oscillation satisfactory (numerical rating of 3).

Dihedral effect.- The data (fig. 13) show that the dihedral effects are greater at low speed. Since swept wings tend to have higher effective dihedral as angle of attack is increased, it is felt that the indicated increase is due to high angles of attack and is not a result of leading-edge BLC flap. At 140 knots the dihedral effect is about the same with the BLC leading-edge flap and the slatted leading edge.

Roll performance.- Figure 20 shows that with the BLC leading-edge flap the roll performance, as measured by the roll parameter pb/2V, was nearly constant in the landing-approach speed range and little different from the slatted leading-edge configuration. The pilots considered the rolling performance satisfactory, with a numerical rating of 2.

Lateral oscillatory characteristics.- The period and damping of the lateral directional oscillation, figure 21, changed little with the replacement of the slatted leading edge with the BLC flap. The data also indicate that the low speed and higher angles of attack achieved with the present configuration changed the period and damping very little. The only comment the pilots made on the lateral characteristics was that at low speed and high angles of attack more effort was required to keep the wings level.

Stalling characteristics.- The stalling speeds of the airplane with slatted leading edge and with BLC leading-edge flaps with varying momentum coefficient, $C_{\mu_{LE}}$, are shown in figure 22. The data are computed from $C_{L_{max}}$ values for the power approach configuration, assuming a gross weight of 22,000 pounds. The stall at values of $C_{\mu_{LE}}$ above about 0.015 was characterized by the following: (1) positive static longitudinal stability throughout the stall maneuver; (2) essentially no roll-off tendency; (3) rapid increase in drag as stall speed was approached; (4) little or no stall warning. The pilots considered the stall characteristics satisfactory but some sort of artificial stall warning would be desirable.

At low values of $C_{\mu_{LE}}$ (below $C_{\mu_{LE}}$ = 0.015) the approach to the stall was characterized by a pitch-up followed by a pitch-down. The pitch-up became more abrupt as $C_{\mu_{LE}}$ was reduced. The pilots considered the speed at which the pitch-up occurred as the "stall" speed for the purpose of landing and take-off. The speed for pitch-up as determined from the static longitudinal stability data (fig. 17) has been computed and is included in figure 22. At speeds below the pitch-up down to $C_{L_{max}}$, the airplane experienced heavy buffet, marginal lateral directional stability, and rapid increase in drag.

CONCLUSIONS

The following conclusions can be made from this investigation of blowing boundary-layer control (BLC) on a leading-edge flap in conjunction with blowing BLC on the trailing-edge flap.

1. Blowing BLC on a leading-edge flap is an effective means of delaying leading-edge separation, enabling the airplane to be flown to higher angles of attack and at lower airspeeds.

2. Compared with the slatted leading-edge configuration the use of the BLC leading-edge flap resulted in a 9-percent decrease in stalling speed with an accompanying 6-percent decrease in landing-approach speed. The average landing-approach speed was 128 percent of the stall speed, and was limited by ability to control flight-path angles and several factors associated with the high angles of attack; these included visibility, adverse trim change with thrust, and low directional stability.

3. The significant effects of leading-edge BLC on the airplane handling characteristics were to remove objectionable buffet, to improve the stalling characteristics, and to maintain static longitudinal stability down to the stall speed.

4. Flight-path control by use of the throttle alone was difficult because of the necessity of shifting the trim angle of attack to compensate for the changes in thrust magnitude.

5. Thrust loss due to bleed air for BLC was reduced while adequate air flow for BLC was maintained by the use of pressure-actuated switches which controlled the BLC ducting valves and kept the duct pressures constant for all engine speeds used in landing approach and at wave-off.

6. The effects of the leading-edge boundary-layer control flap on the lift and drag characteristics of the airplane were as predicted from wind-tunnel tests.

Ames Research Center
    National Aeronautics and Space Administration
        Moffett Field, Calif., March 9, 1960

APPENDIX

LIFT AND DRAG CHARACTERISTICS

Effect of Leading-Edge BLC on Maximum Lift, Flap Lift, and Drag

Figure 23(a) presents the lift curves and drag polars for the airplane with and without leading-edge BLC for the trailing-edge BLC flaps both up and down. The figure also shows for comparative purposes the lift and drag data for the airplane with the slatted leading edge (ref. 1). These data show that large increases in $C_{L_{max}}$ and angle of attack for $C_{L_{max}}$ are possible with leading-edge BLC flaps. The flap lift is also slightly higher in terms of C_L for a given α except at the low C_L values.

Figure 23(b) presents the lift curves and drag polars of the airplane with various amounts of leading-edge blowing ($C_{\mu_{LE}}$) while a fixed variation of $C_{\mu_{TE}}$ with C_L is maintained. These data show that as $C_{\mu_{LE}}$ was increased, the lift curve slope above $\alpha \approx 12^\circ$ increased resulting in higher maximum lifts, but there was little change in the angle of attack for maximum lift. Figure 24 shows the variation of maximum lift with $C_{\mu_{LE}}$.

The drag for the leading-edge flap configuration is lower than for the slatted leading edge (fig. 23(a)). The amount of drag reduction depends on $C_{\mu_{LE}}$ as shown in figure 23(b). The reduction in drag at lift and momentum coefficients used in the landing approach was approximately equal to the thrust loss due to bleed air for leading-edge BLC.

Comparison of Flight With Wind-Tunnel Lift and Drag Data

Figure 25 compares the variation of C_L with α and the drag polars as determined in the full-scale wind tunnel and in flight. The wind-tunnel data were part of the investigation of reference 2 and the trimmed-lift data were computed for a center-of-gravity position, similar to that of the airplane, in terms of percent MAC. The main difference between the two tests was the difference in fuselage and the fact that C_μ in the wind-tunnel data was constant, while $C_{\mu_{LE}}$ in flight varied from 0.004 to 0.020 and $C_{\mu_{TE}}$ varied from 0.004 to 0.017. The data show good correlation in the variation of C_L with α at C_L values above about 1.1. The differences below C_L of about 1.1 can partially be attributed to the higher flap effectiveness in the wind tunnel due to the use of higher $C_{\mu_{TE}}$ than in flight.

The drag coefficient at a given lift coefficient as measured in the wind tunnel was about 0.04 higher than in flight, but the general shapes of the drag polars were similar.

REFERENCES

1. Quigley, Hervey C., Anderson, Seth B., and Innis, Robert C.: Flight Investigation of the Low-Speed Characteristics of a $45°$ Swept-Wing Fighter-Type Airplane With Blowing Boundary-Layer Control Applied to the Trailing-Edge Flaps. NACA RM A58E05, 1958.

2. Maki, Ralph L.: Low-Speed Wind-Tunnel Investigation of Blowing Boundary-Layer Control on Leading- and Trailing-Edge Flaps of a Large Scale, Low-Aspect-Ratio, $45°$ Swept-Wing Airplane Configuration. NASA MEMO 1-23-59A, 1959.

3. Anderson, Seth B., Cooper, George E., and Faye, Alan E., Jr.: Flight Measurements of the Effect of a Controllable Thrust Reverser on the Flight Characteristics of a Single-Engine Jet Airplane. NASA MEMO 4-26-59A, 1959.

4. Drinkwater, Fred J., III, and Cooper, George: A Flight Evaluation of the Factors Which Influence the Selection of Landing Approach Speeds. NASA MEMO 10-6-58A, 1958.

5. White, Maurice D., Schlaff, Bernard A., and Drinkwater, Fred J., III: A Comparison of Flight-Measured Carrier-Approach Speeds With Values Predicted by Several Different Criteria for 41 Fighter-Type Airplane Configurations. NACA RM A57L11, 1958.

6. White, Maurice D., and Innis, Robert C.: A Flight Investigation of the Low-Speed Handling Qualities of a Tailless Delta-Wing Fighter Airplane. NASA MEMO 4-15-59A, 1959.

A
3
5
3

TABLE I.- GEOMETRIC DATA OF AIRPLANE

```
Wing
  Airfoil section . . . . . . . . . . . . . . . . . . . . . . . . NACA 64A007
  Total area, sq ft . . . . . . . . . . . . . . . . . . . . . . . . 400.2
  Span, ft  . . . . . . . . . . . . . . . . . . . . . . . . . . . . 38.8
  Mean aerodynamic chord, ft  . . . . . . . . . . . . . . . . . . . 11.2
  Taper ratio . . . . . . . . . . . . . . . . . . . . . . . . . . . 0.26
  Aspect ratio  . . . . . . . . . . . . . . . . . . . . . . . . . . 3.72
  Sweep at 0.25 chord line, deg . . . . . . . . . . . . . . . . . . 45
  Incidence . . . . . . . . . . . . . . . . . . . . . . . . . . . . 0
  Dihedral  . . . . . . . . . . . . . . . . . . . . . . . . . . . . 0
  Aileron
    Area, sq ft . . . . . . . . . . . . . . . . . . . . . . . . . . 37.0
    Travel, deg . . . . . . . . . . . . . . . . . . . . . . . . . . ±15
  Flap
    Area, sq ft . . . . . . . . . . . . . . . . . . . . . . . . . . 29.8
    Chord, percent wing chord, average  . . . . . . . . . . . . . . 25.0
Horizontal tail
  Airfoil section . . . . . . . . . . . . . . . . . . . . . . . NACA 65A003.5
  Total area, sq ft . . . . . . . . . . . . . . . . . . . . . . . . 98.9
  Span, ft  . . . . . . . . . . . . . . . . . . . . . . . . . . . . 18.7
  Sweep at 0.25 chord line, deg . . . . . . . . . . . . . . . . . . 45.0
  Travel
    Leading edge up, deg  . . . . . . . . . . . . . . . . . . . . . 4.0
    Leading edge down, deg  . . . . . . . . . . . . . . . . . . . . 25.0
Vertical tail
  Airfoil section . . . . . . . . . . . . . . . . . . . . . . . NACA 65A003.5
  Total area, sq ft . . . . . . . . . . . . . . . . . . . . . . . . 45.2
  Area, rudder, sq ft . . . . . . . . . . . . . . . . . . . . . . . 6.3
  Span, ft  . . . . . . . . . . . . . . . . . . . . . . . . . . . . 7.9
  Sweep, deg  . . . . . . . . . . . . . . . . . . . . . . . . . . . 45
```

A
3
5
3

TABLE II.- PILOT OPINION RATING SYSTEM

Operation	Adjective rating	Numerical rating	Description	Primary mission accomplished	Can be landed
Normal operation	Satisfactory	1	Excellent, includes optimum	Yes	Yes
		2	Good, pleasant to fly	Yes	Yes
		3	Satisfactory, but with some mildly unpleasant characteristics	Yes	Yes
Emergency operation	Unsatisfactory	4	Acceptable, but with unpleasant characteristics	Yes	Yes
		5	Unacceptable for normal operation	Doubtful	Yes
		6	Acceptable for emergency condition only[1]	Doubtful	Yes
No operation	Unacceptable	7	Unacceptable even for emergency condition[1]	No	Doubtful
		8	Unacceptable – dangerous	No	No
		9	Unacceptable – uncontrollable	No	No
	Catastrophic	10	Motions possibly violent enough to prevent pilot escape	No	No

[1]Failure of a stability augmenter

TABLE III.- SUMMARY OF LANDING APPROACH SPEEDS WITH COMMENTS

Pilot	Slatted leading edge (ref. 1)		BLC leading-edge flap		
	V_A, knots	V_A/V_s	V_A, knots	V_A/V_s	Reason for limiting
A	135.0	1.24	126.5	1.31	Primary: Limits of the ability to control longitudinal flight path
B	136.5	1.26	126.5	1.31	Secondary: Visibility, trim change with thrust, static directional stability, sluggish longitudinal control
C	130.0	1.20	120.5	1.23	
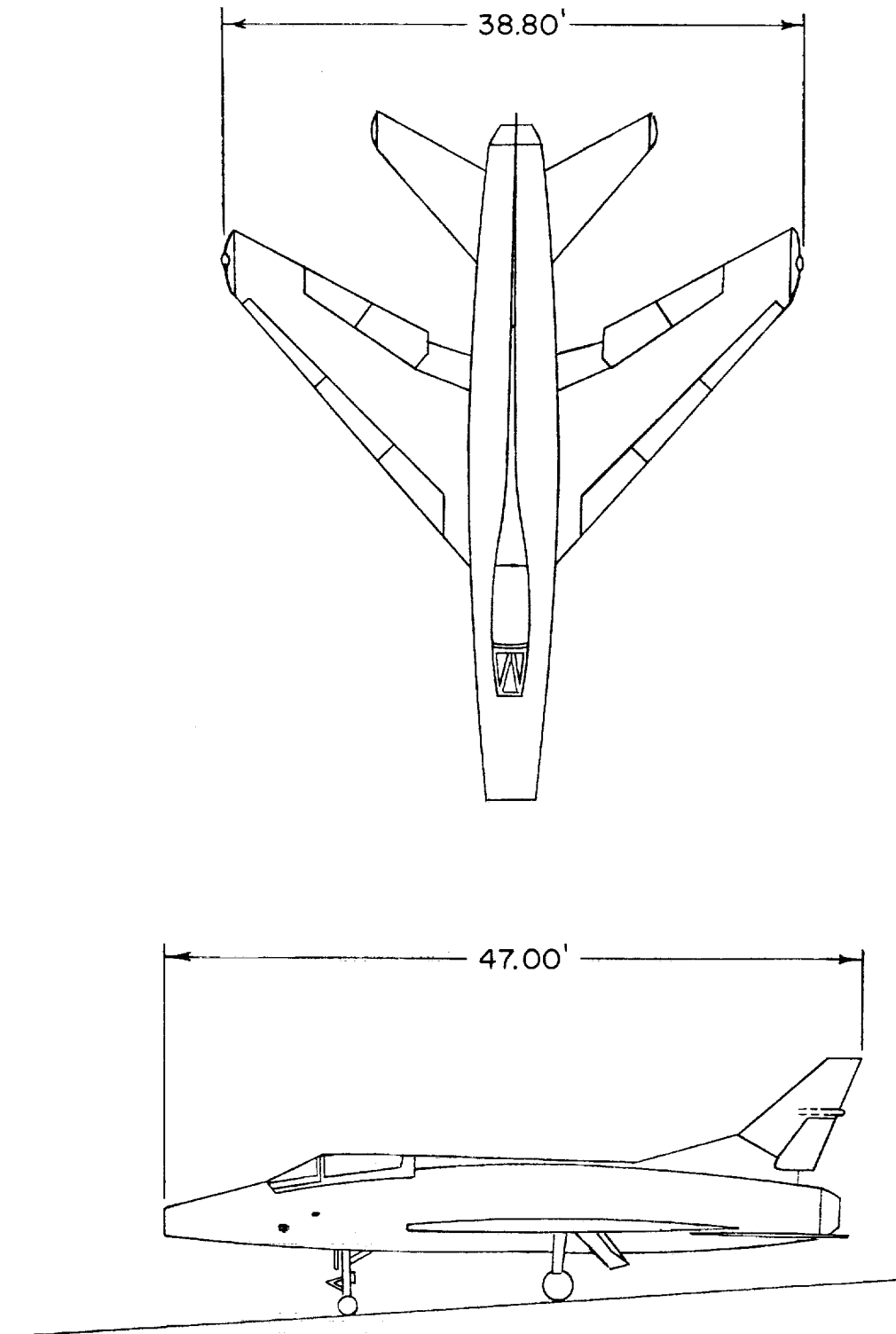
Figure 1.- Two-view drawing of test airplane.
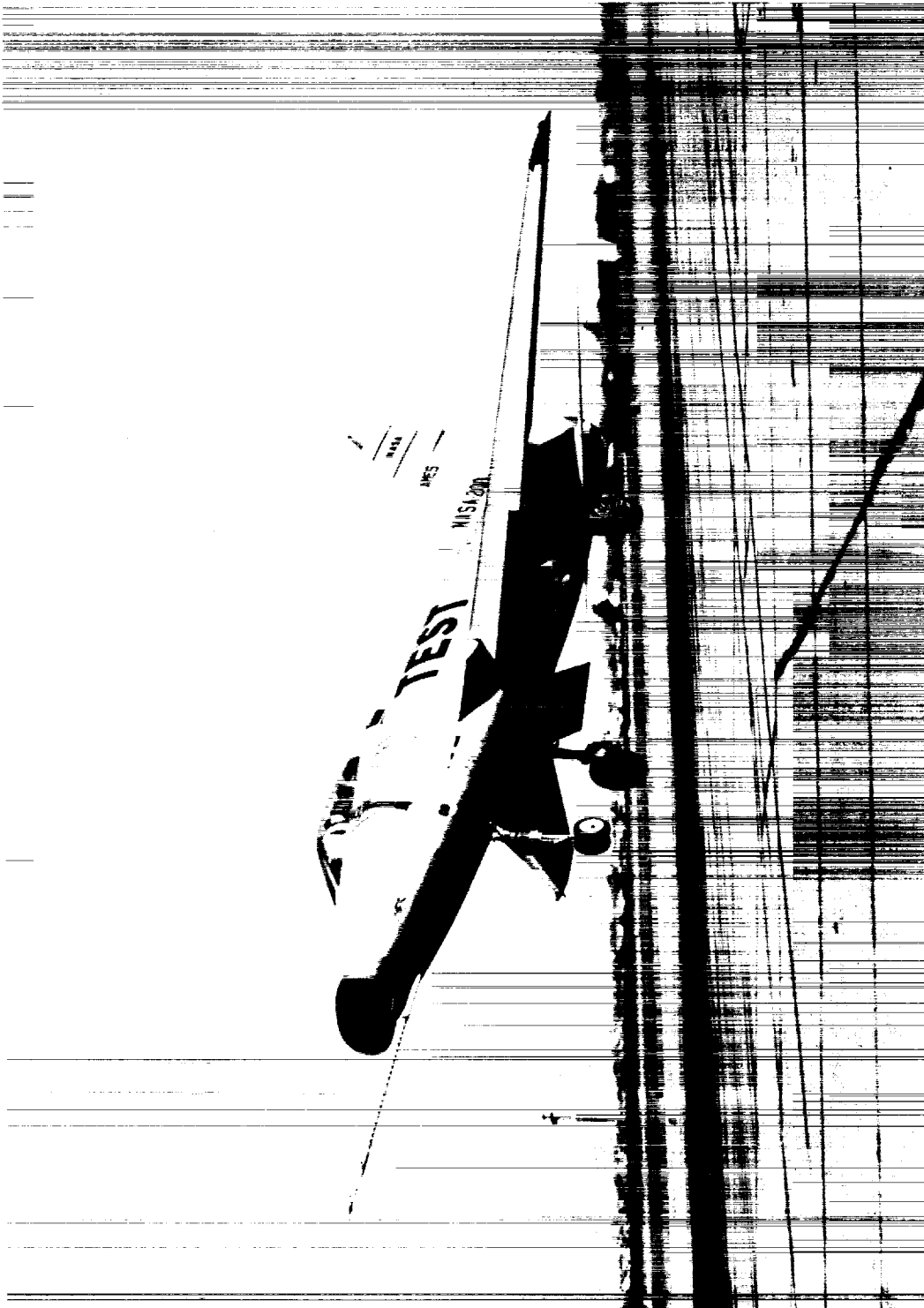
Figure 2.- Photograph of test airplane.

A-24696
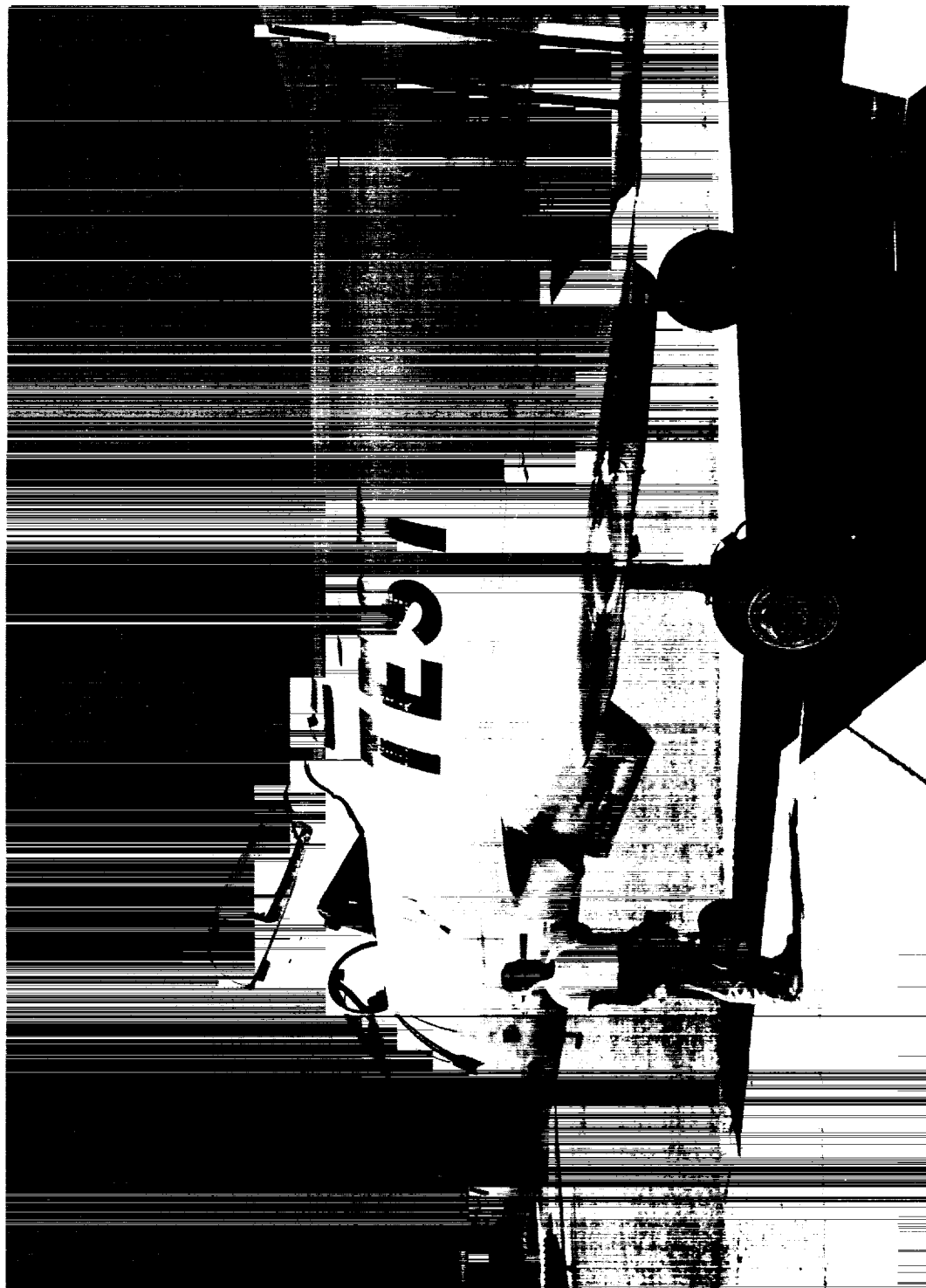
A-24041

Figure 3.- Photograph of leading-edge boundary-layer control flap.

Nozzle

Duct
2.9" I.D.   20.9 to 45.0 % b/2
2.4" I.D.   46.2 to 79.6 % b/2
1.4" I.D.   82.0 to 97.6 % b/2

30°

60°

Center of
flap rotation

Flap position
link
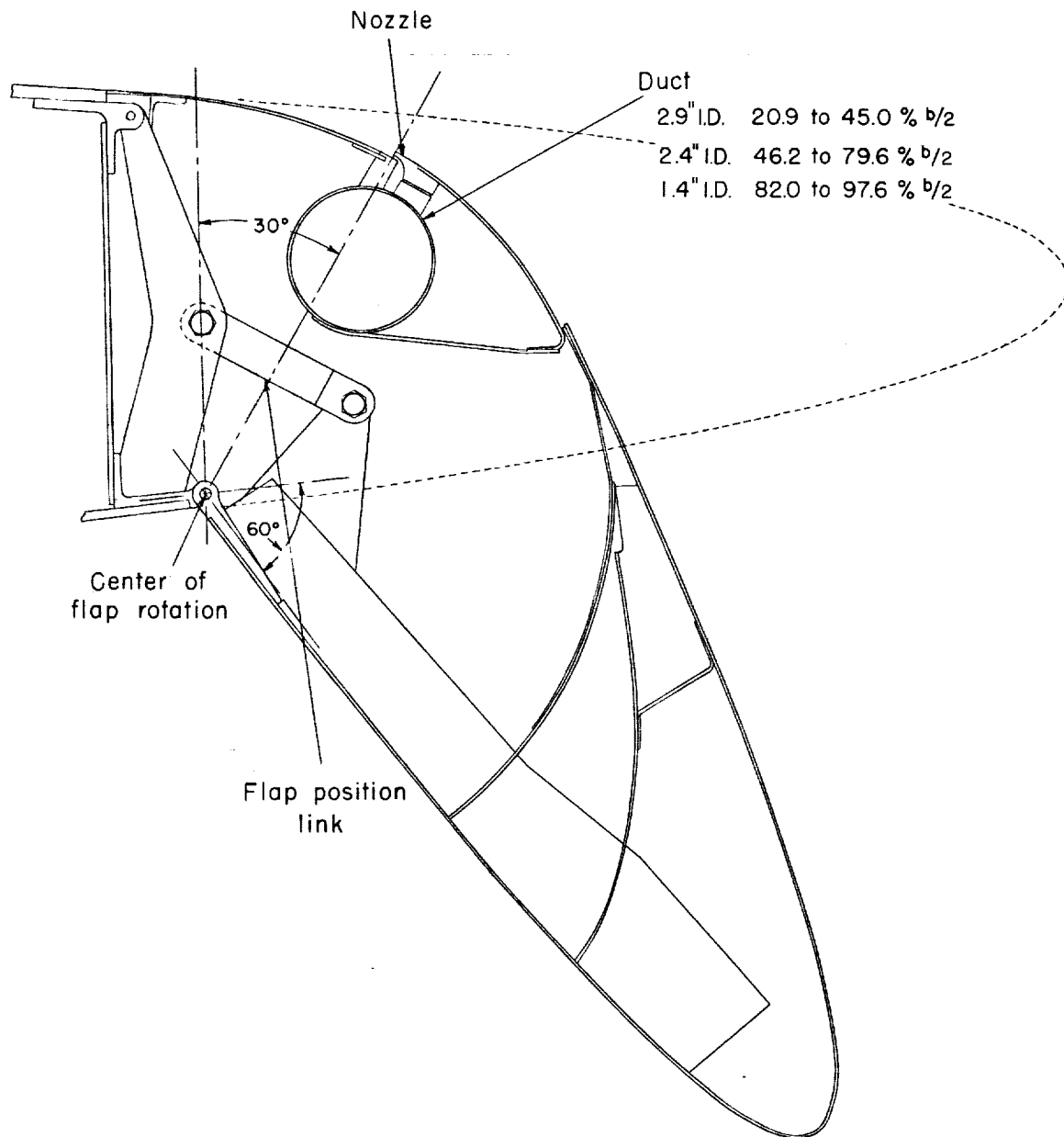
A
3
5
3

(a) Cross section.

Figure 4.- Sketch of leading-edge boundary-layer control flap details.

$\mathsf{¢}$
Fus.

94.5 % $b/2$

65.0 % $b/2$

44° 08'

40.0 % $b/2$

23.2 % $b/2$

20.9 % $b/2$

Nose flap hinge plane

14.3 % $b/2$

0% $b/2$
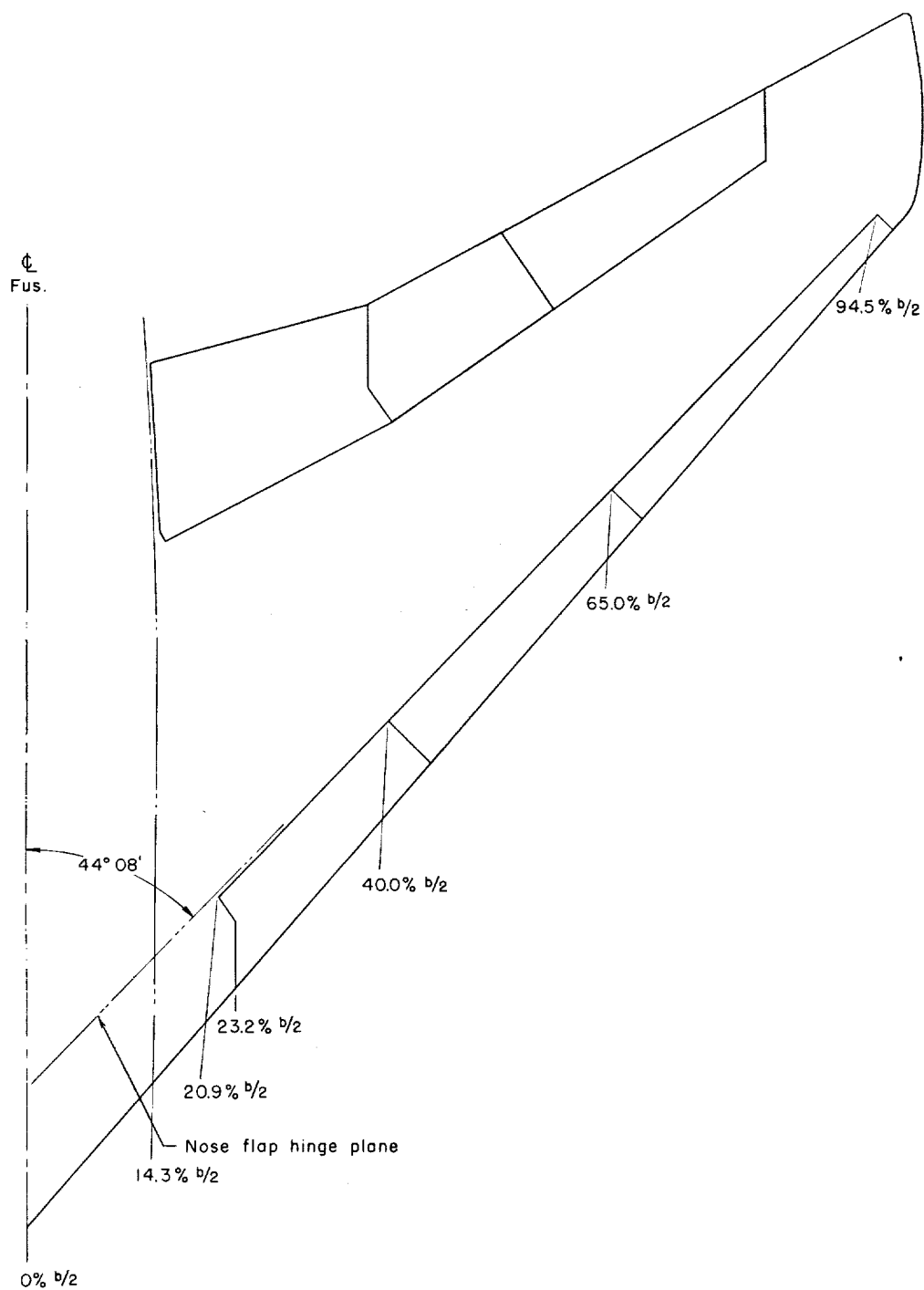
(b) Plan form.

Figure 4.- Concluded.

COLLECTOR RING

T.E. BLEED AIR
CONTROL VALVE

BLOWING NOZZLE

L.E. BLEED AIR
CONTROL VALVE

DUCT

BLEED AIR
CONTROL SWITCHES

L.E. / T.E.

OPEN
OFF
CLOSED

MAN.
AUTO.

A
3
5
3
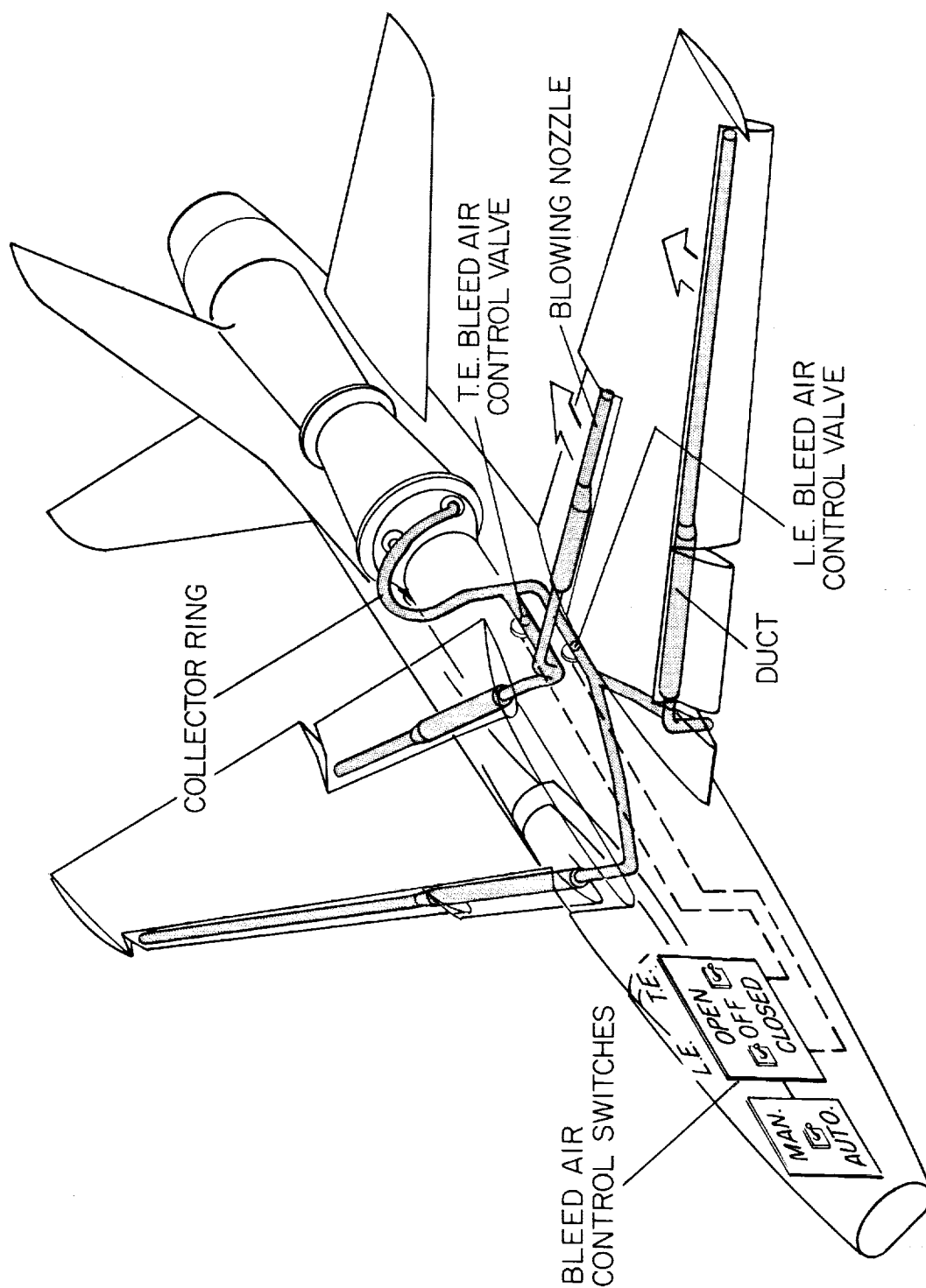
Figure 5.- Sketch of bleed air ducting.

Figure 6.- Photograph of underfuselage ducting.

A-24040
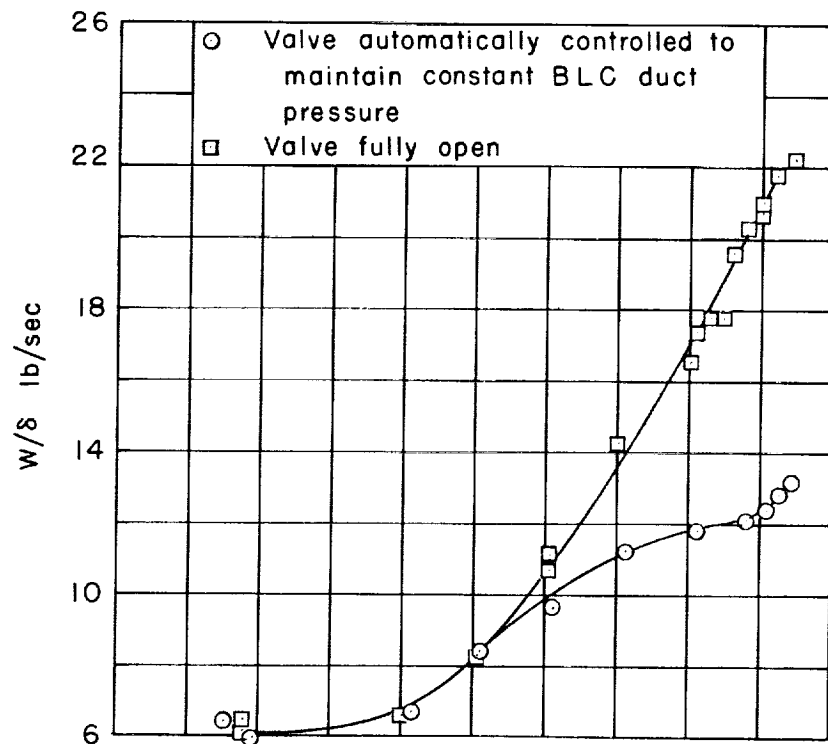
(a) Total bleed air flow, LE and TE.
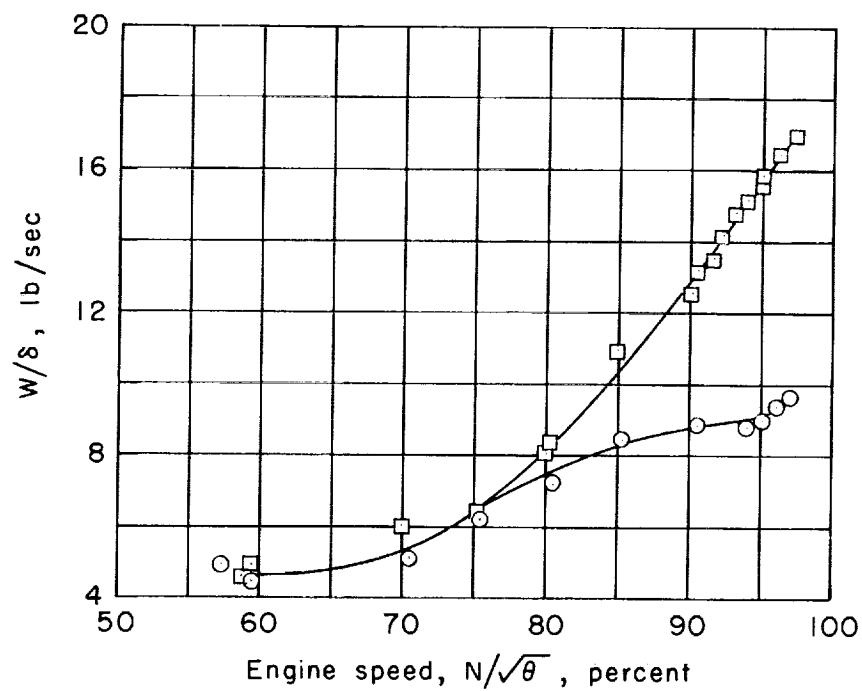
(b) Bleed air flow to LE.

Figure 7.- Variation of bleed air flow for BLC with engine speed.
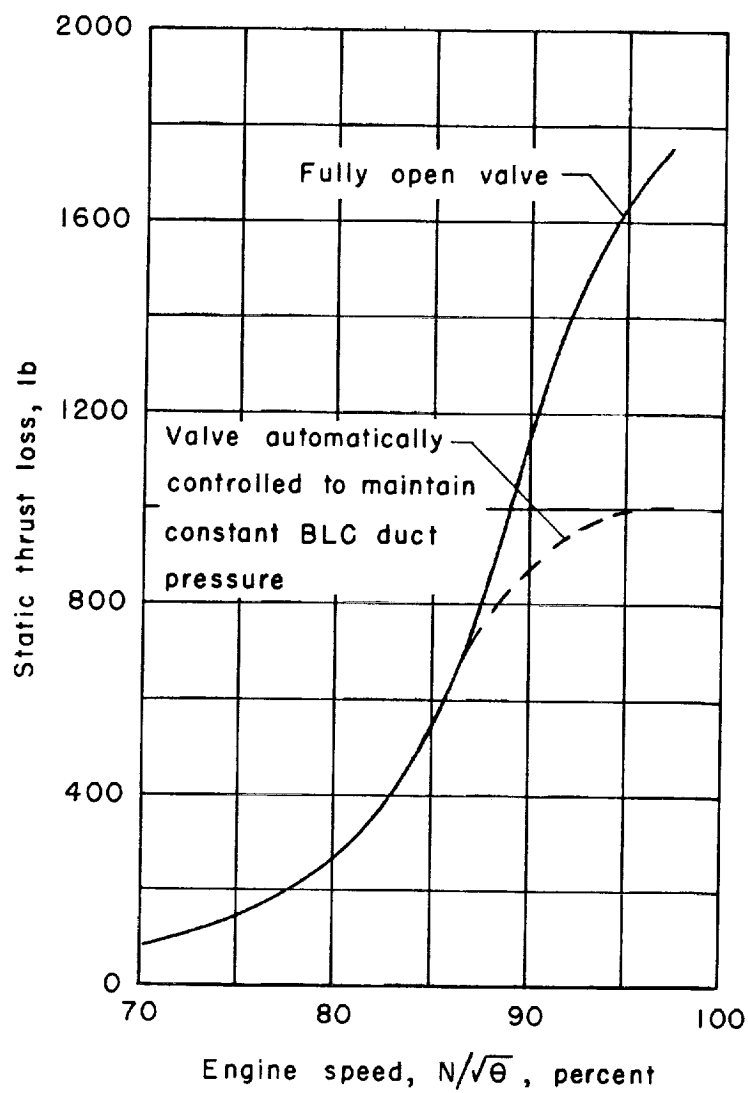
Figure 8.- Variation of thrust loss due to engine bleed air for boundary-
layer control with engine speed.
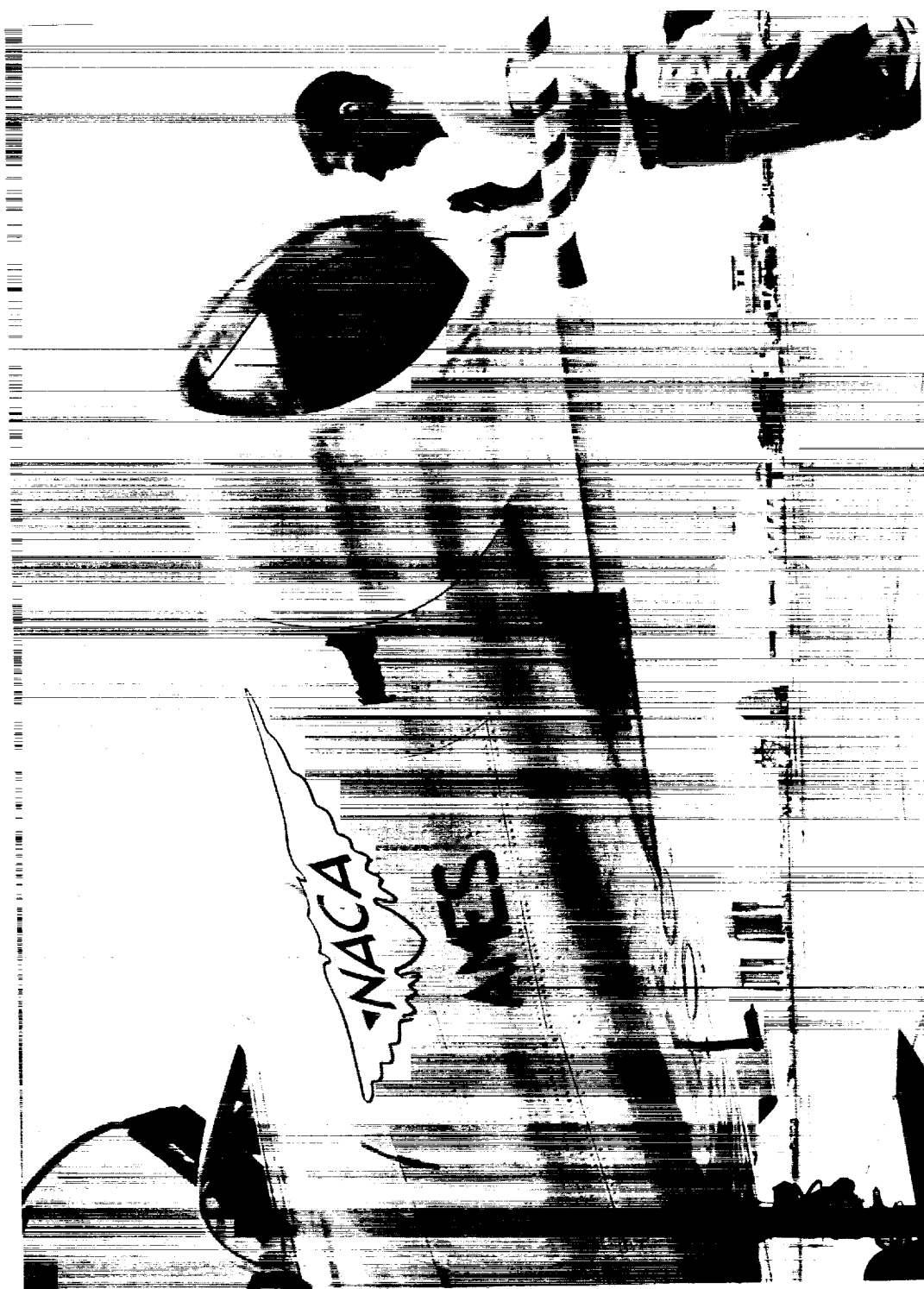
A-24039

Figure 9.- Modified inlet.

A
3
5
3

A
3
5
3
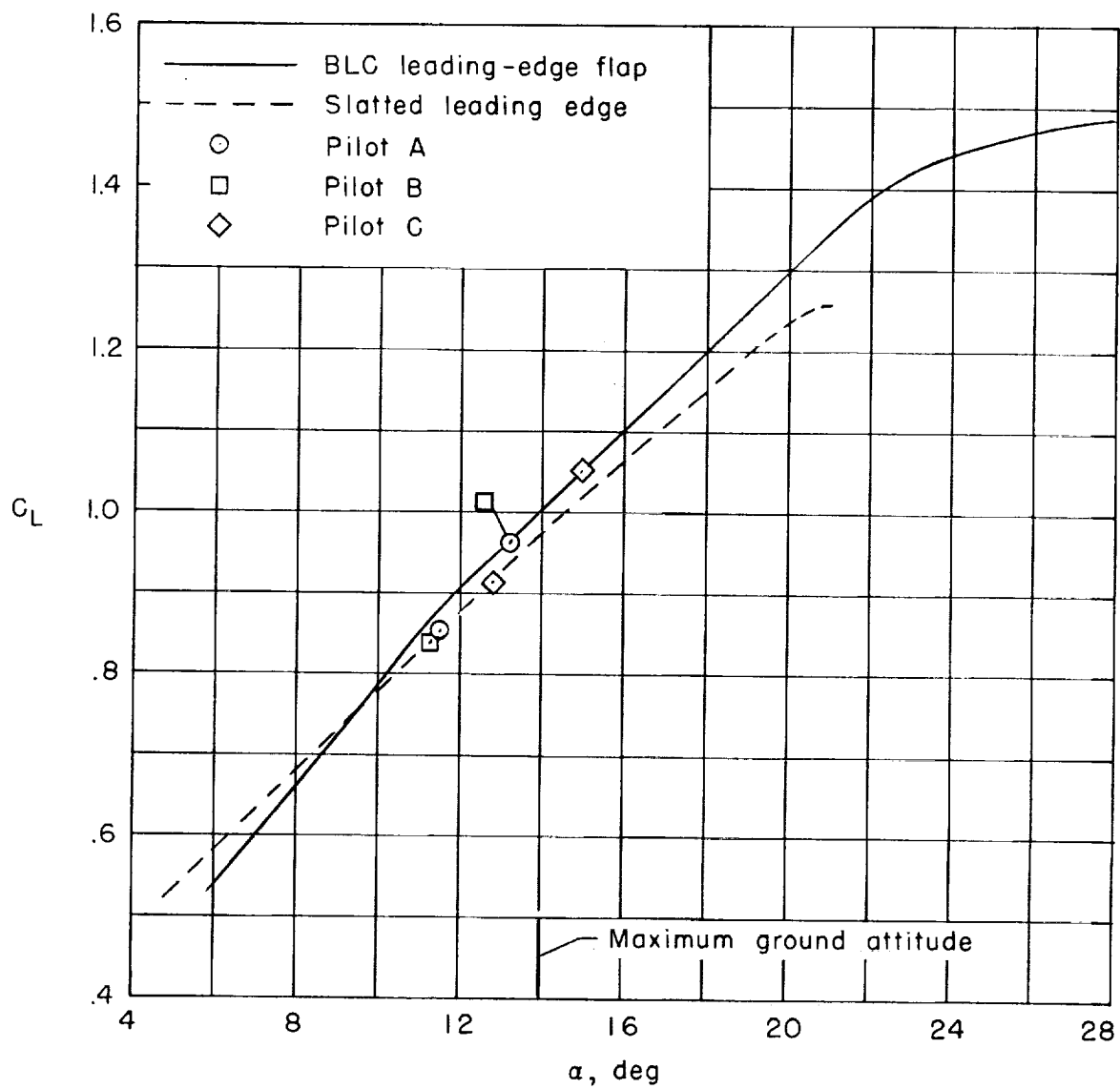
Figure 10.- Relationship of pilots' approach speed to lift curves.

Oleo fully extended

14°
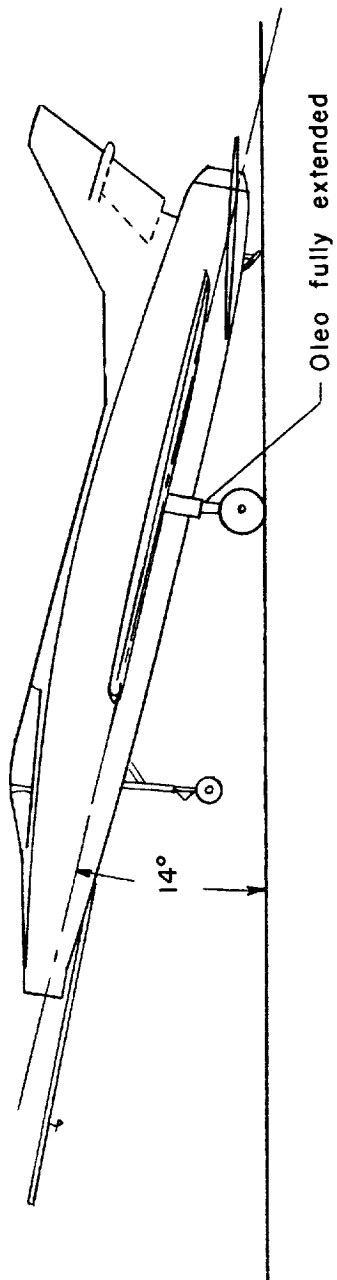
Figure 11.- Sketch showing maximum ground angle of airplane at touchdown.

A
3
5
3
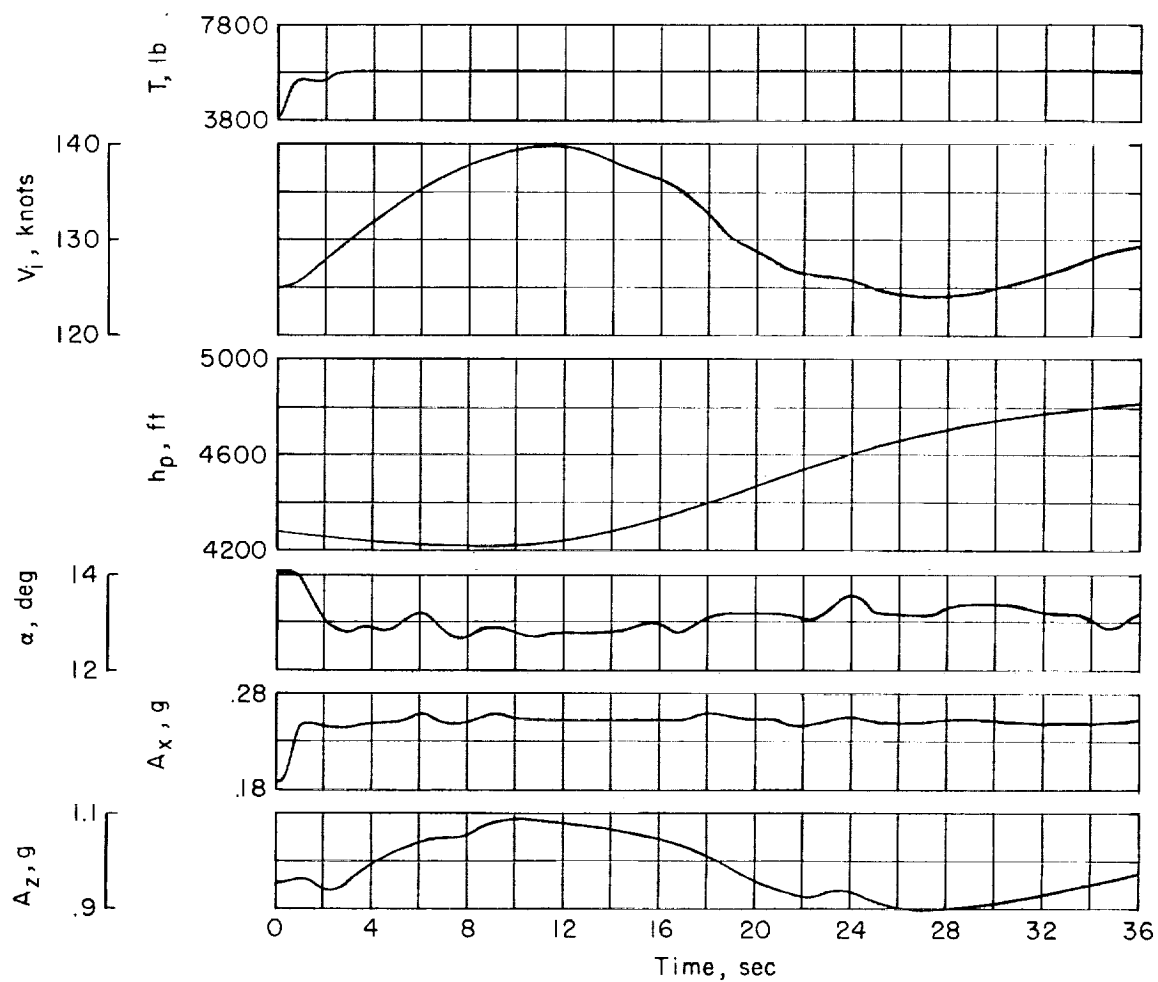
(a) Time history of throttle step; $\delta_f = 45^\circ$ with BLC, δ_t constant.

Figure 12.- Airplane response and trim characteristics with thrust changes.
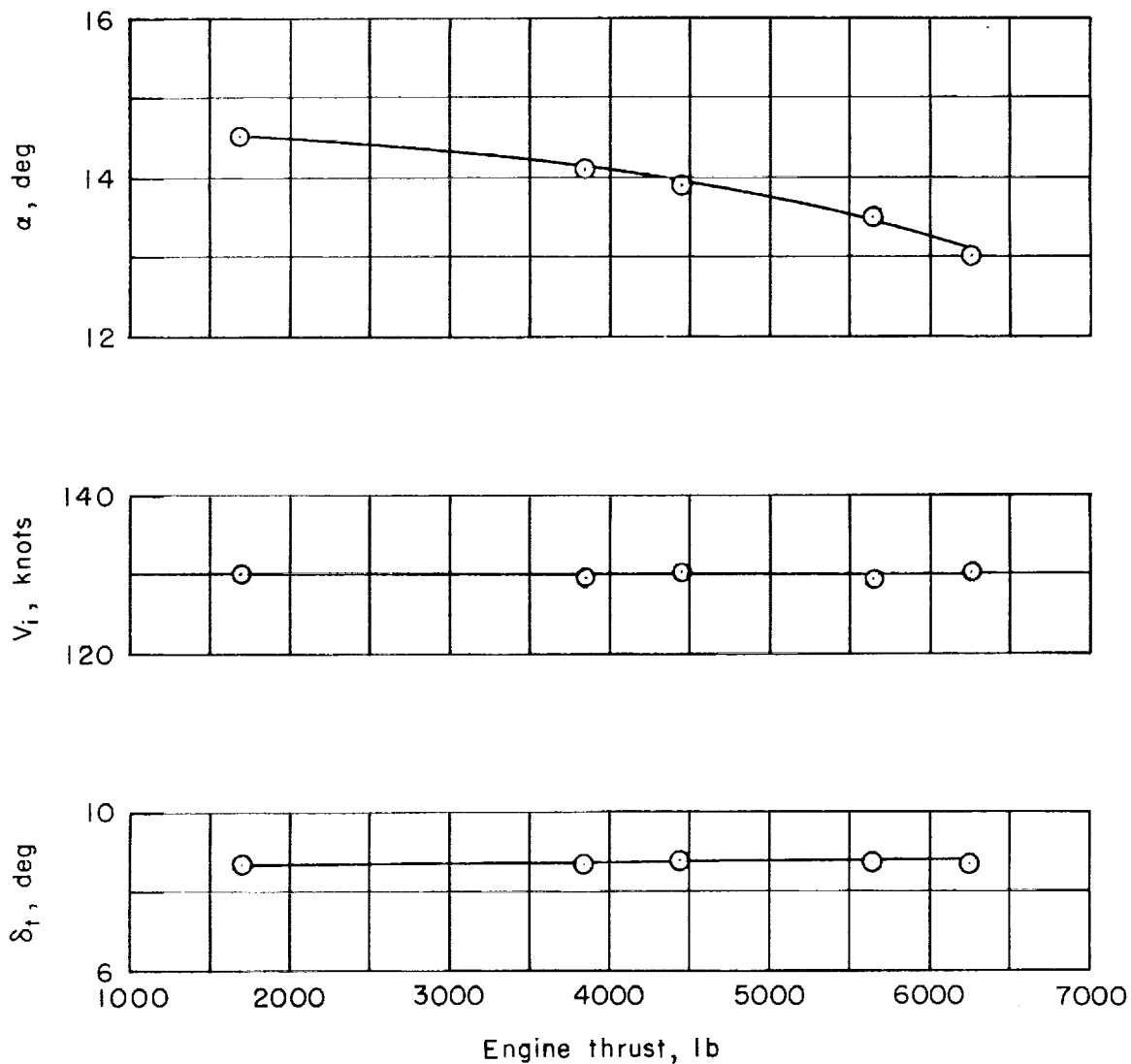
(b) Trim angle of attack and horizontal-tail angle variation with engine thrust at 130 knots.

Figure 12.- Concluded.
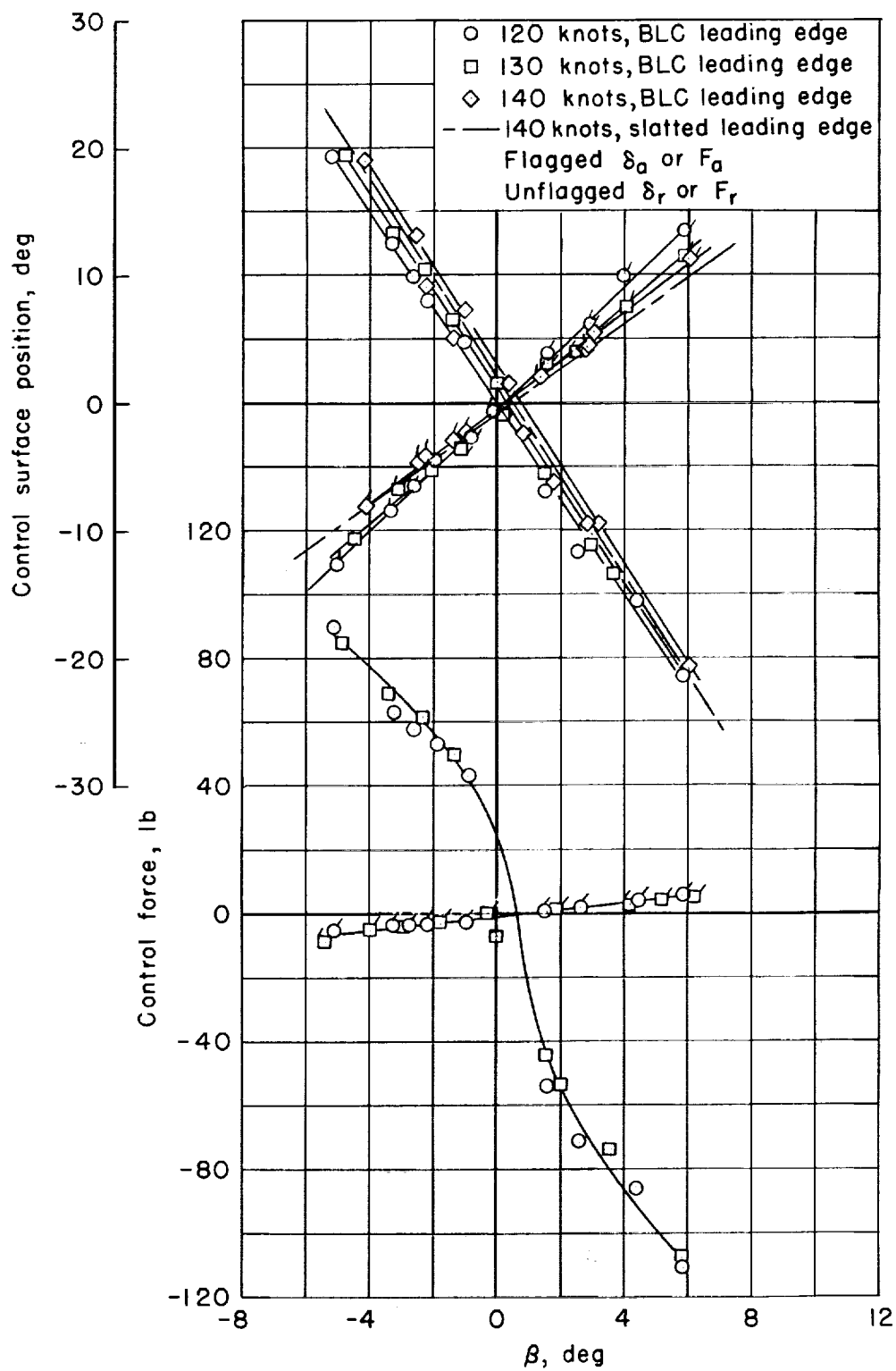
Figure 13.- Static directional stability and dihedral effect.
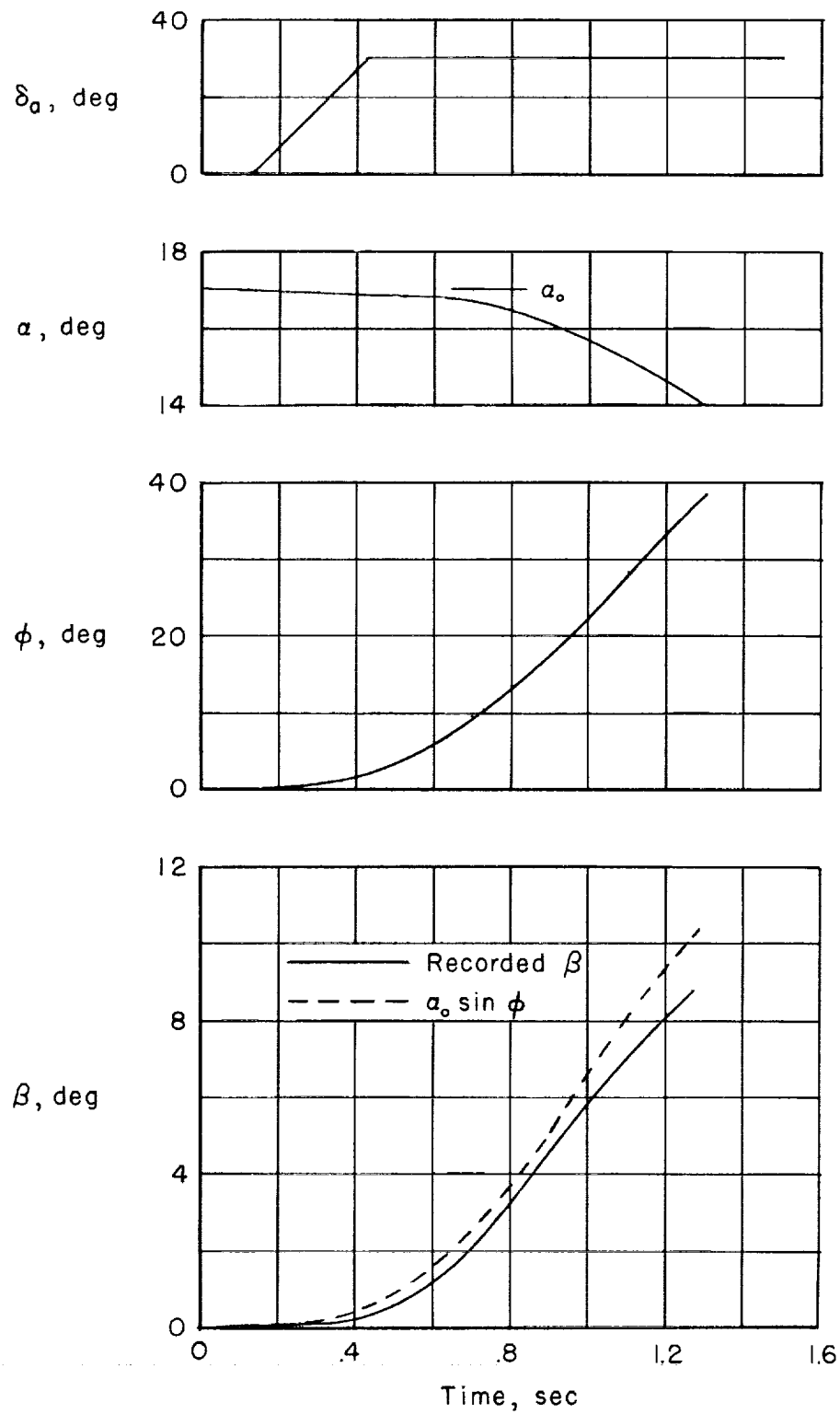
Figure 14.- Time history of full aileron roll; V_i = 120 knots.
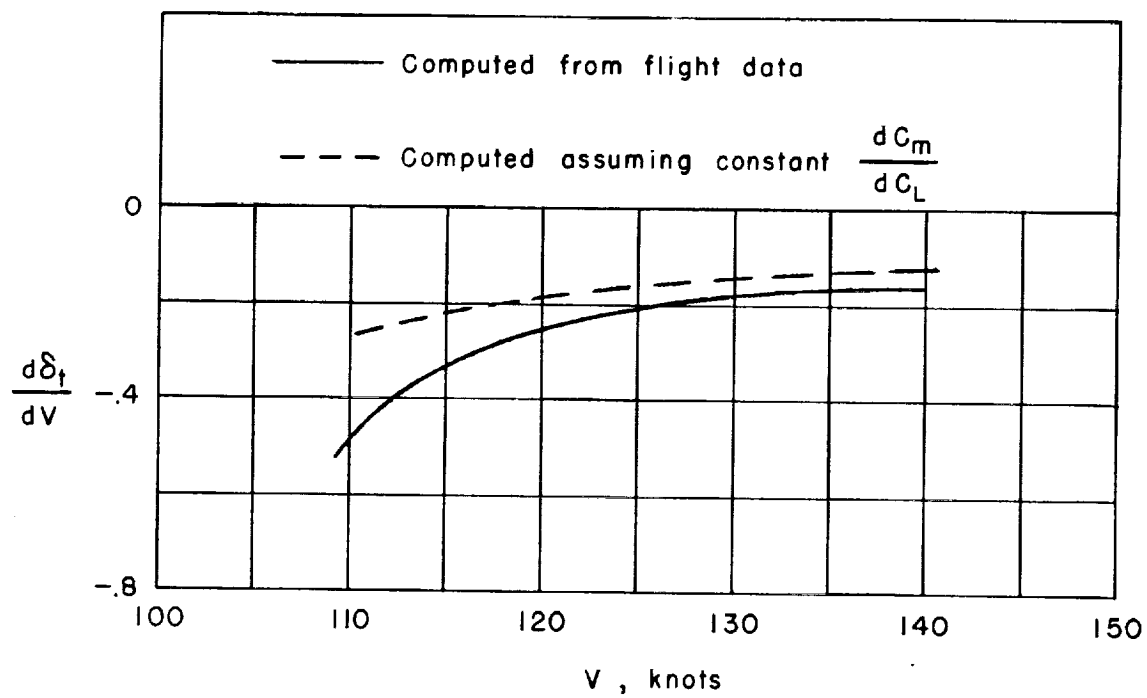
Figure 15.- Variation of the static longitudinal stability parameter, $d\delta_t/dV$ with airspeed.
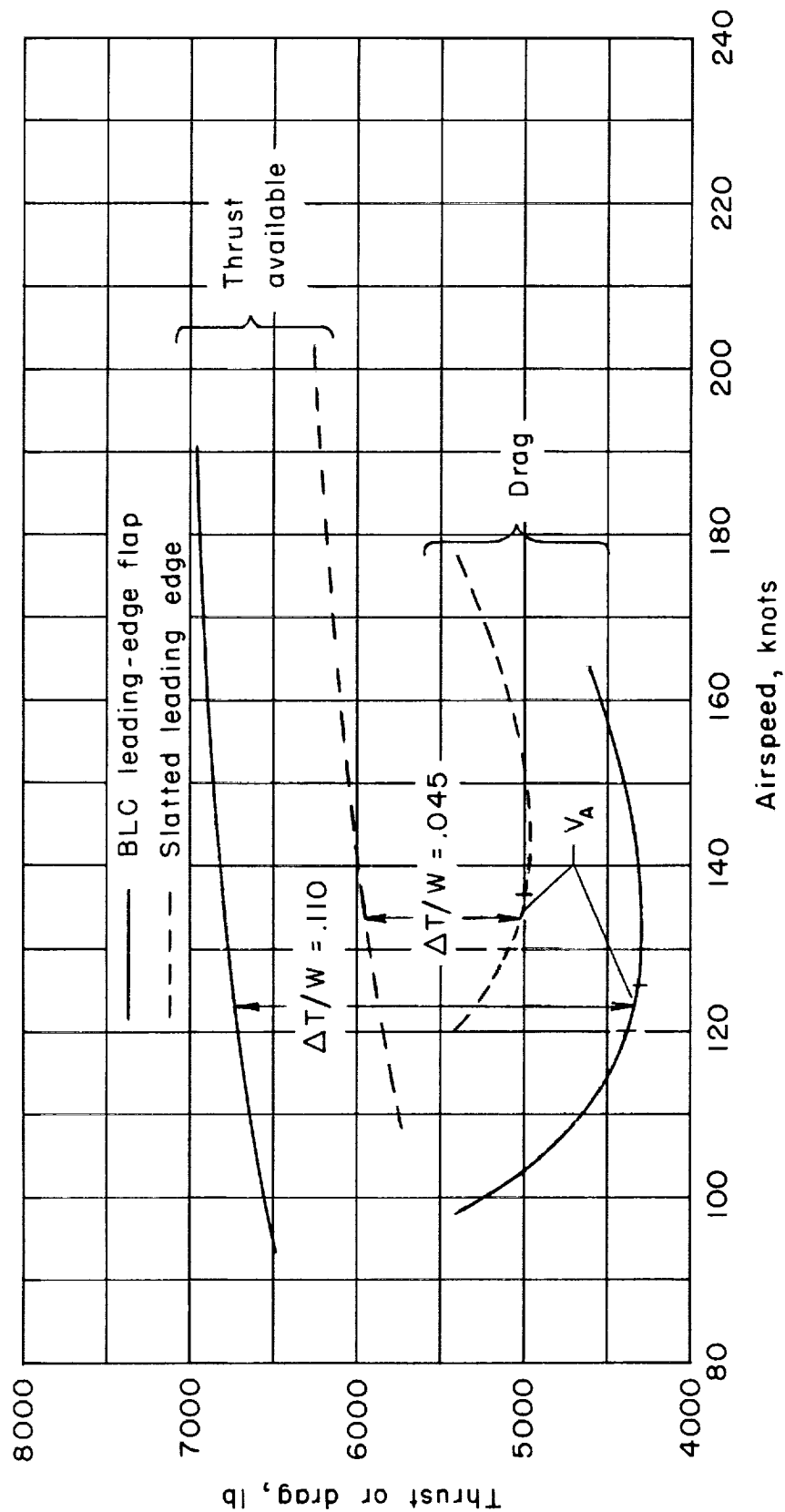
Figure 16.- Variation of drag and thrust available with airspeed; weight, 22,000 pounds.

A
3
5
3
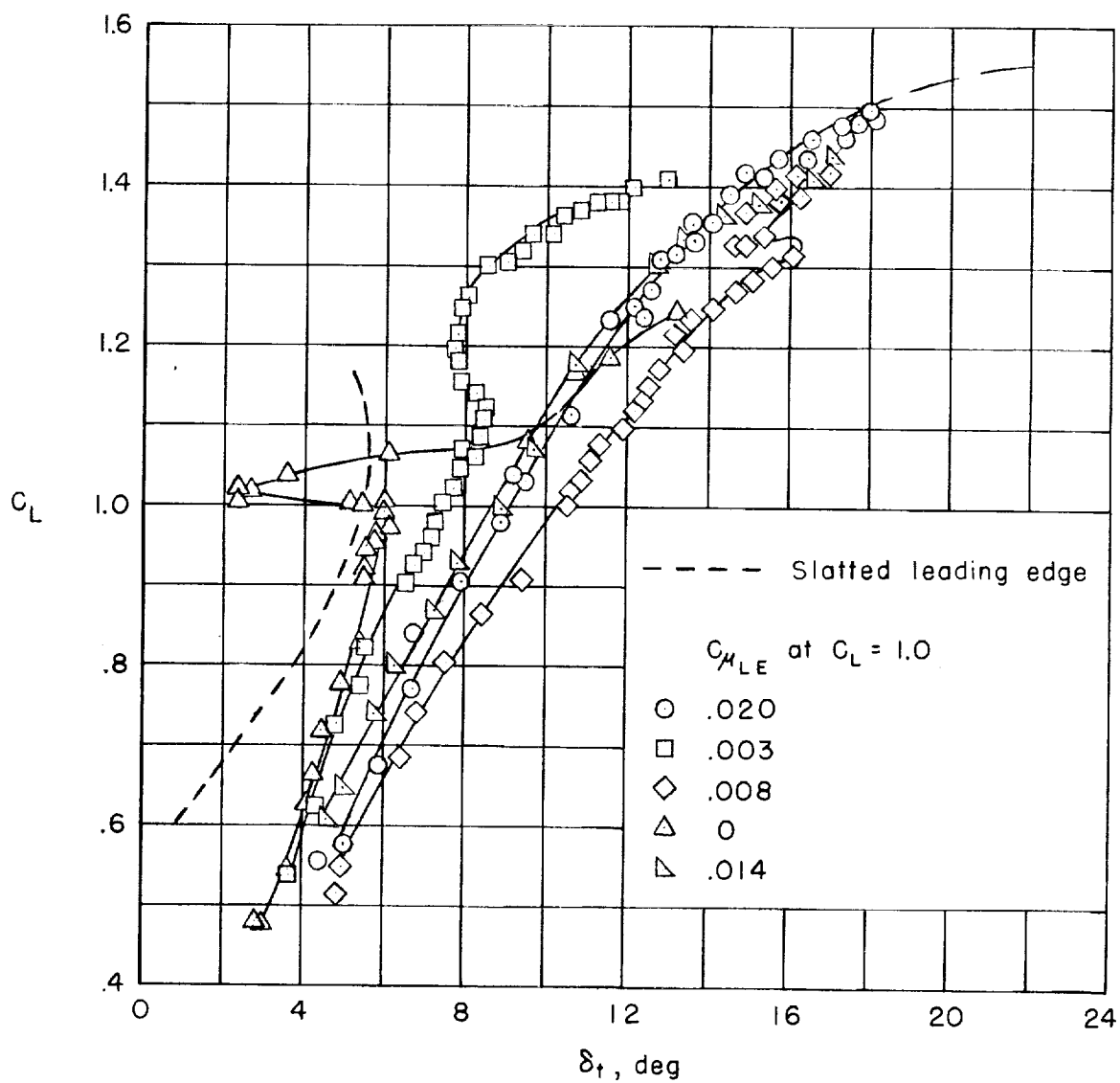
Figure 17.- Variation of the lift coefficient with the tail angle required
for trim for various amounts of leading-edge blowing.
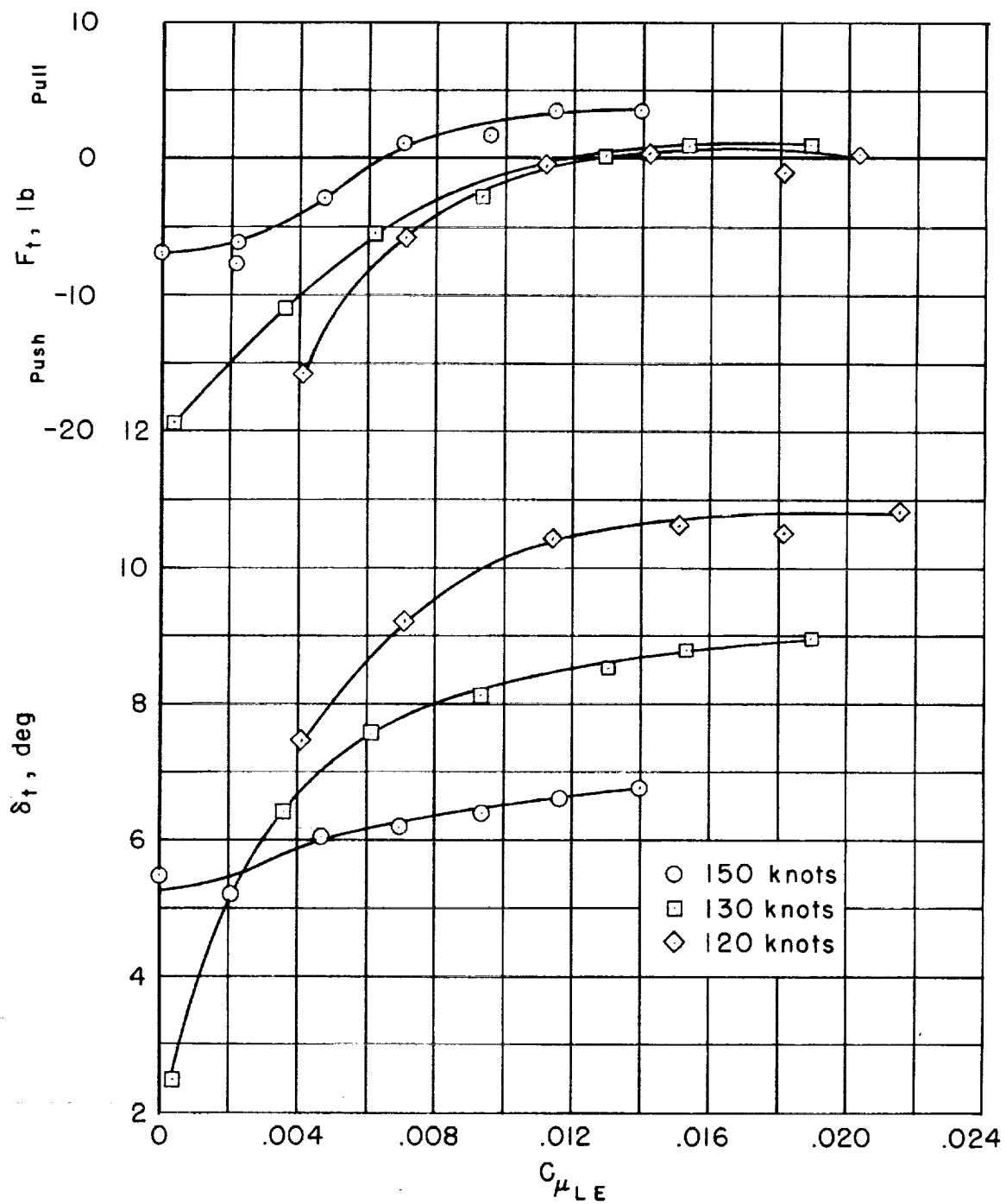
Figure 18.- Trim change due to leading-edge BLC; $C_{\mu_{TE}}$ constant.

A
3
5
3
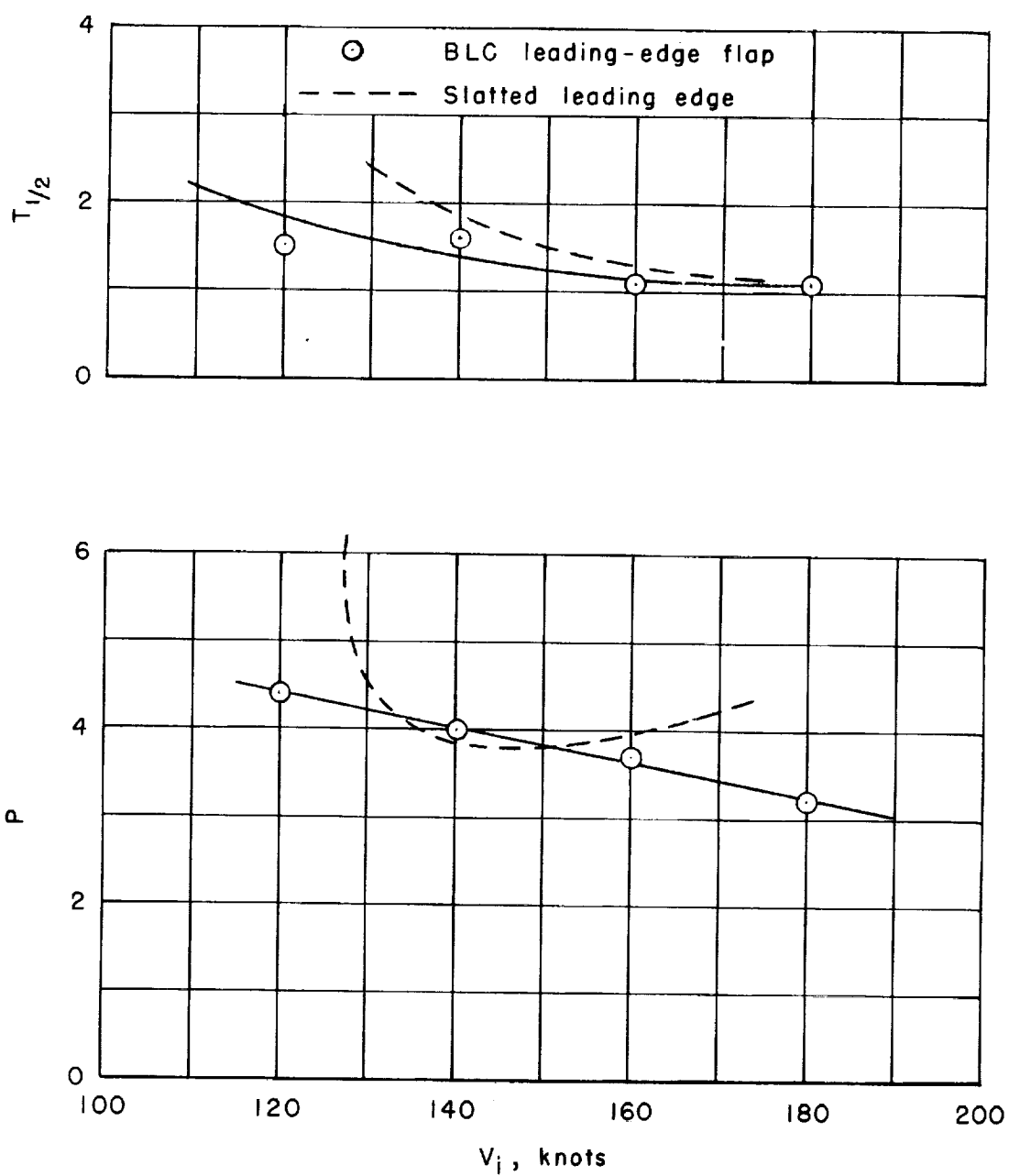
Figure 19.- Dynamic longitudinal stability.
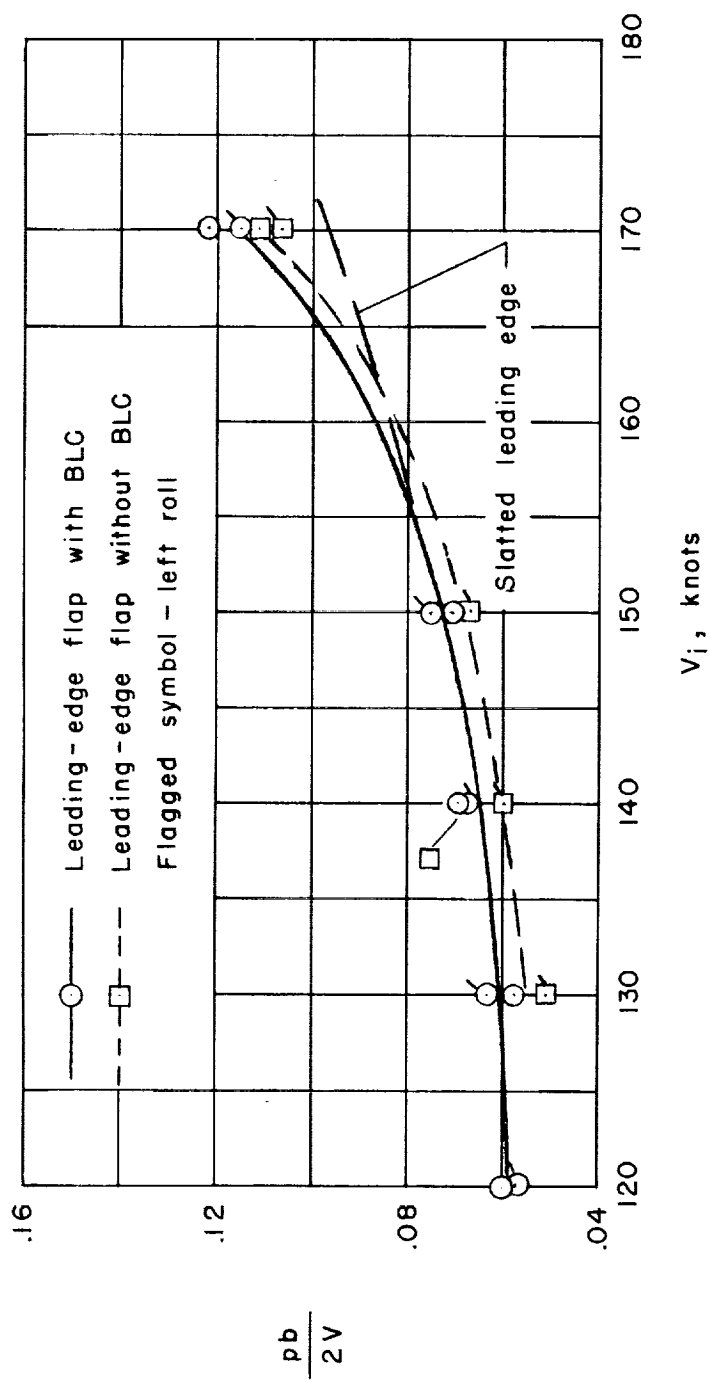
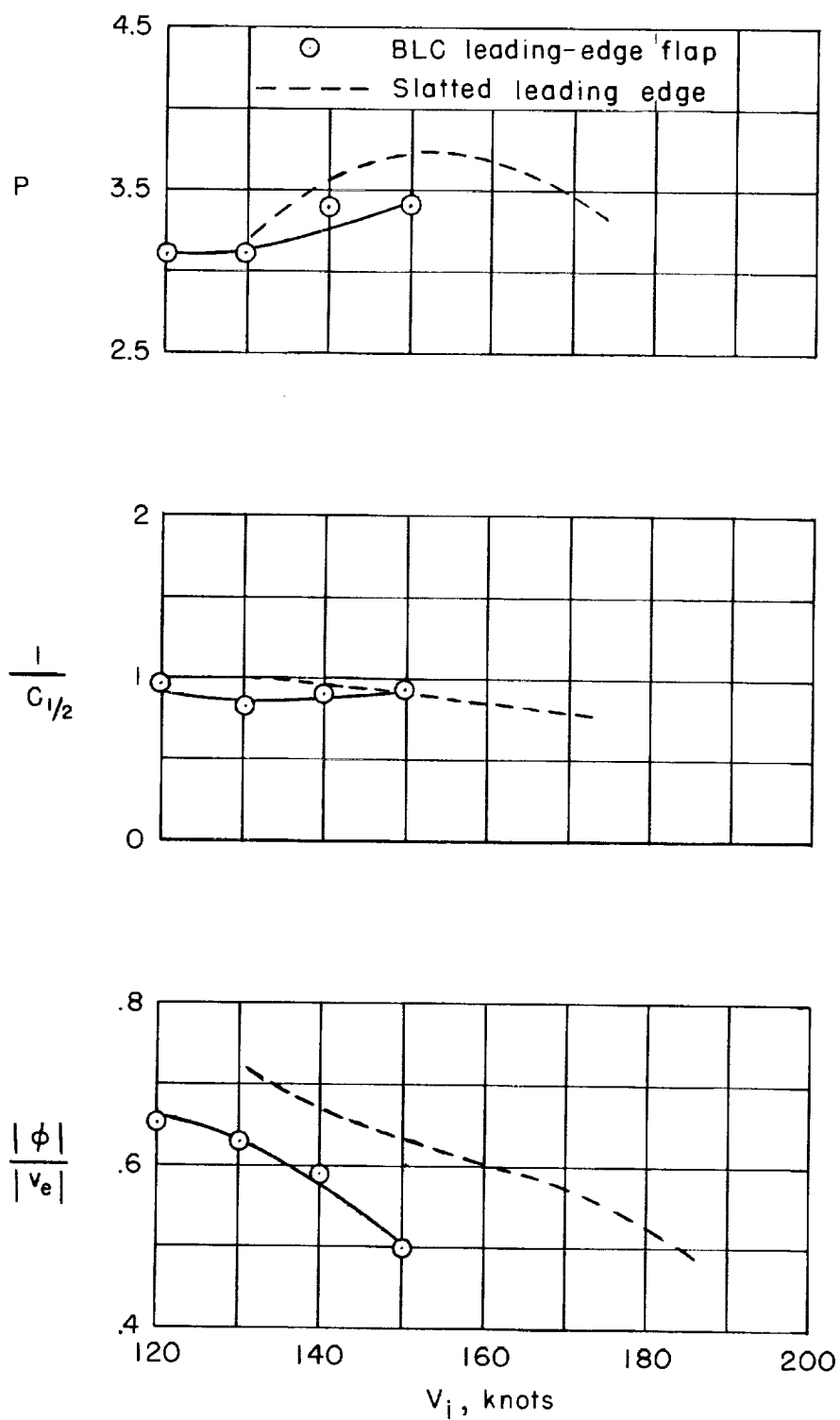Figure 20.- Rolling performance with maximum aileron deflection; $\delta_a = 30°$.
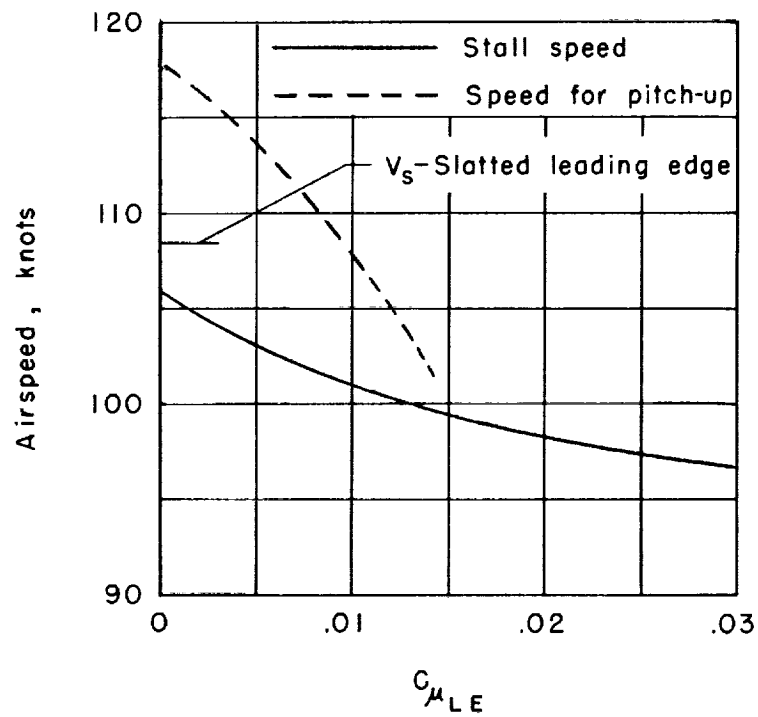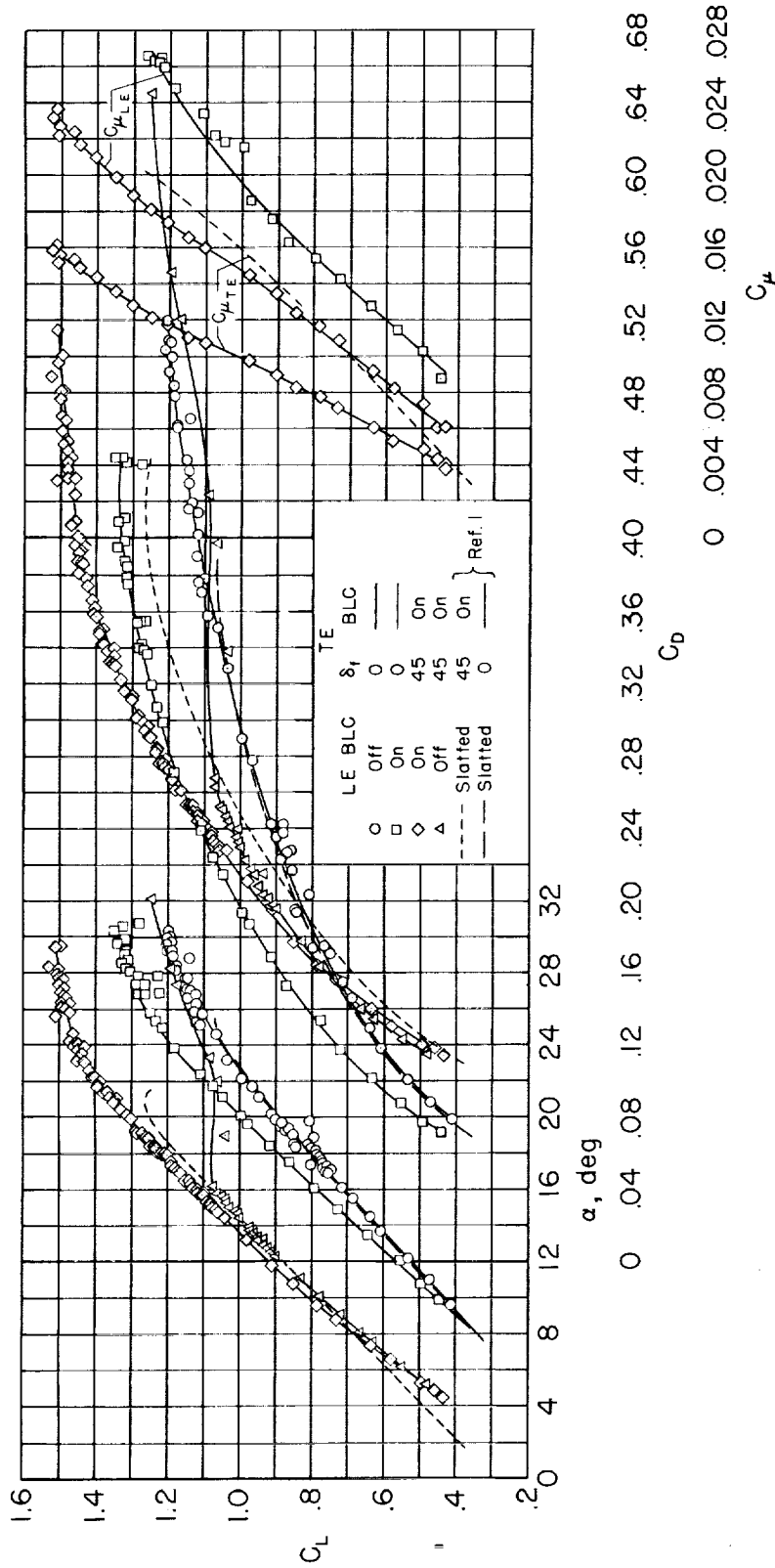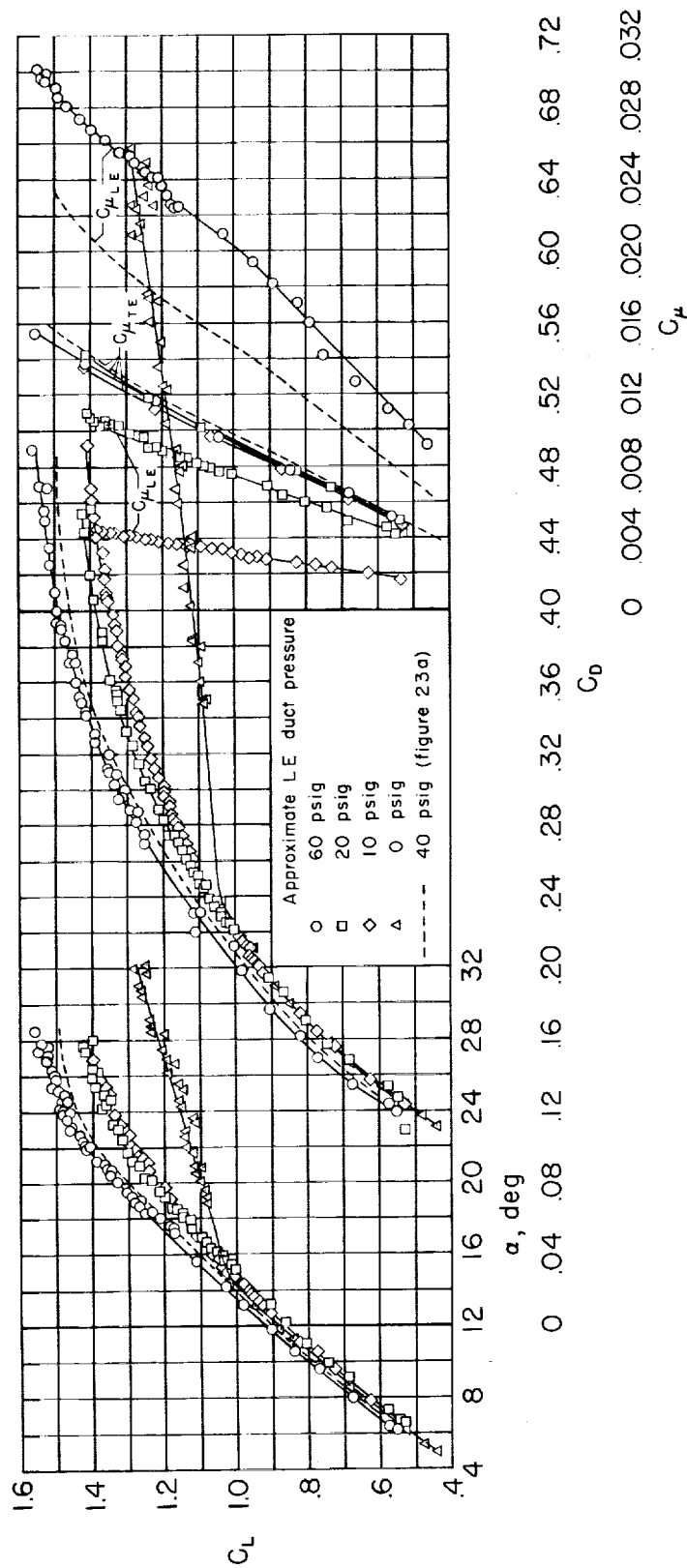
Figure 21.- Lateral oscillatory characteristics.

Figure 22.- Variation of minimum speed with leading-edge C_μ, 22,000 pounds gross weight.

(a) Various configurations with BLC on and off.

Figure 23.- Lift and drag characteristics for various configurations and momentum coefficients.

42

Approximate L E duct pressure

○ 60 psig
□ 20 psig
◇ 10 psig
△ 0 psig
----- 40 psig (figure 23a)

$C_{\mu_{LE}}$

$C_{\mu_{TE}}$

C_L

1.6
1.4
1.2
1.0
.8
.6
.4

α, deg

8 12 16 20 24 28 32

0 .04 .08 .12 .16 .20 .24 .28 .32 .36 .40 .44 .48 .52 .56 .60 .64 .68 .72

C_D

0 .004 .008 .012 .016 .020 .024 .028 .032

C_μ

(b) Various amounts of leading-edge momentum coefficient.
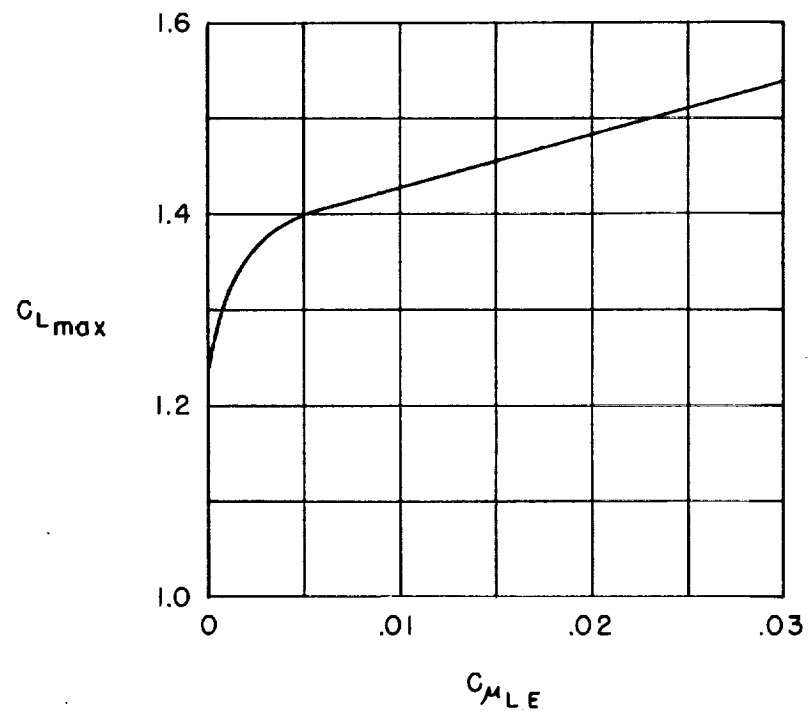
Figure 23.- Concluded.

A
3
5
3

A
3
5
3

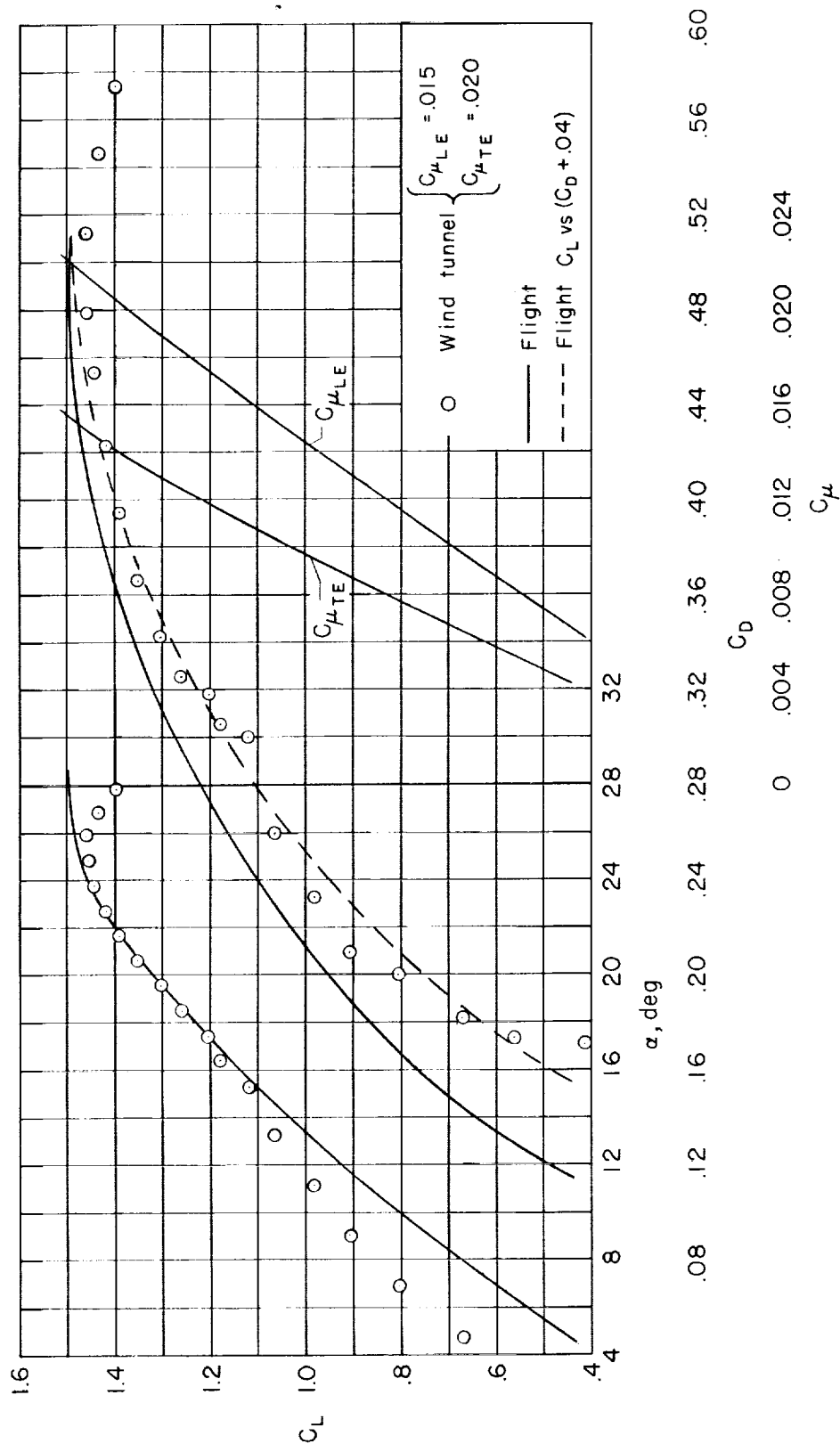Figure 24.- Variation of maximum lift coefficient with momentum coefficient.

Figure 25.- Correlation of flight and wind-tunnel lift and drag characteristics.